Unravelling structural, functional, evolutionary and genetic basis of SWEET transporters regulating abiotic stress tolerance in maize

P.N. Vinodh Kumar [a,b], Mallana Gowdra Mallikarjuna [a,*], Shailendra Kumar Jha [a], Anima Mahato [b], Shambhu Krishan Lal [c], Yathish K.R. [d], Hirenallur Chandappa Lohithaswa [e], Viswanathan Chinnusamy [f]

[a] Division of Genetics, ICAR - Indian Agricultural Research Institute, New Delhi 110012, India
[b] ICAR - Indian Agricultural Research Institute, Jharkhand, India
[c] School of Genetic Engineering, ICAR - Indian Institute of Agricultural Biotechnology, Ranchi 834003, India
[d] Winter Nursery Centre, ICAR-Indian Institute of Maize Research, Hyderabad, India
[e] Department of Genetics and Plant Breeding, University of Agricultural Sciences, GKVK, Bengaluru 560065, India
[f] Division of Plant Physiology, ICAR- Indian Agricultural Research Institute, New Delhi 110012, India

A B S T R A C T

Sugars Will Eventually be Exported Transporters (SWEETs) are the novel sugar transporters widely distributed among living systems. SWEETs play a crucial role in various bio-physiological processes, viz., plant developmental, nectar secretion, pollen development, and regulation of biotic and abiotic stresses, in addition to their prime sugar-transporting activity. Thus, in-depth structural, evolutionary, and functional characterization of maize SWEET transporters was performed for their utility in maize improvement. The mining of *SWEET* genes in the latest maize genome release (*v.5*) showed an uneven distribution of 20 *ZmSWEETs*. The comprehensive structural analyses and docking of ZmSWEETs with four sugars, viz., fructose, galactose, glucose, and sucrose, revealed frequent amino acid residues forming hydrogen (asparagine, valine, serine) and hydrophobic (tryptophan, glycine, and phenylalanine) interactions. Evolutionary analyses of SWEETs showed a mixed lineage with 50–100 % commonality of ortho-groups and -sequences evolved under strong purifying selection (Ka/Ks < 0.5). The duplication analysis showed non-functionalization (*ZmSWEET18* in B73) and neo- and sub-functionalization (*ZmSWEET3, ZmSWEET6, ZmSWEET9, ZmSWEET19,* and *ZmSWEET20*) events in maize. Functional analyses of *ZmSWEET* genes through co-expression, in silico expression and qRT-PCR assays showed the relevance of *ZmSWEETs* expression in regulating drought, heat, and waterlogging stress tolerances in maize. The first ever *ZmSWEET*-regulatory network revealed 286 direct (*ZmSWEET*-TF: 140 *ZmSWEET*-miRNA: 146) and 1226 indirect (TF-TF: 597; TF-miRNA: 629) edges. The present investigation has given new insights into the complex transcriptional and post-transcriptional regulation and the regulatory and functional relevance of *ZmSWEETs* in assigning stress tolerance in maize.

1. Introduction

Sugars are the major source of carbon and energy for synthesizing several intermediates of the metabolic pathways in higher plants [1]. The sugar molecules fuel the cellular carbon and energy metabolism through the storage and transport of nutrients and play an essential role in signal transduction and resistance to various stresses [1–4]. In plants, sugars are mainly synthesized during photosynthesis in leaves through solar energy assisted conversion of CO_2 into organic carbon [5,6]. The efficient transportation and distribution of sugars from source to sink organs, viz. fruits, grains, roots etc., is mediated by specialized proteins called sugar transporters. These sugar transporters are crucial for developing sink tissues and providing positive feedback to source tissues to ensure adequate energy allocation and sustain the trade-off between the different organs [2,5–7]. Hence, sugar transporters in the plant system act as bridges to connect the cellular exchange of carbon and energy to execute various biological functions [6].

The SWEET (Sugars Will Eventually be Exported Transporter) family

is a newly characterized group of sugar transporters, which are generally localized to the plasma membranes, and their primary function is to regulate the influx and the efflux of sugar into and out of cells. It has been showed that typical eukaryotic SWEET proteins comprise seven α-helical transmembrane (TM) domains organized as tandem repeats of two 3-1-3 fashion, i.e., 3 TM domains (containing two conserved MtN3/ saliva motifs: PF03083) that are separated by a single TM that is less conserved [8,9]. Thus, the structure is popularly known as the 3-1-3 TM SWEET structure [10]. Nevertheless, recently the presence of 14 TMHs was shown in an ExtraSWEET protein of *Vitis vinifera* [11].

In plants, the SWEETs play various functional roles, viz. phloem transport, nectar secretion, pollen nutrition, stress tolerance, and plant-pathogen interactions [10,12]. Several SWEET genes regulating developmental and stress tolerance were characterized and cloned in many plant species, including maize. The seed filling in cultivated maize and rice is controlled by *ZmSWEET4c* (maize) and *OsSWEET4* (rice) through hexose transport across the basal endosperm transfer layer [13]. During host-pathogen interactions, the SWEET genes act as targets for effector proteins, which allows the pathogens to modify the expression of *SWEETs* to gain sugars to fuel their growth and reproduction [2,14]. Thus, SWEET genes are known as susceptibility (S) genes. In rice, *Xa13/ OsSWEET11*, *Xa25/OsSWEET13*, and *OsSWEET14* were identified as targets of *Xanthomonas oryzae* pv. *oryzae* effectors [15–17]. Similarly, during *Xanthomonas citri* subsp. *malvacearum* invasion in cotton, *GhSWEET10* expression is activated by a TAL effector of pathogen *Avr6* [18].

Abiotic stresses usually trigger significant sugar accumulation in plant tissues. Therefore, SWEET proteins play an important role in regulating abiotic stress tolerance. In Arabidopsis, the overexpression of *AtSWEET15* resulted in accelerated leaf senescence and showed hypersensitivity to high salinity stress whereas, the deficient mutant lines with *atsweet15* are less sensitive to high salinity stress [19]. Similarly, the double mutant lines with *atsweet11;12* exhibited greater freezing tolerance than the wild-type and single mutants [20].

Many studies on genome-wide identification and functional characterization of plant *SWEET* gene families are available, viz. Arabidopsis, alfalfa, rice, cucumber, wheat, rubber tree, sweet orange, soybean, tomato, potato, sorghum, pineapple, Chinese cabbage etc. [21]. Focused efforts on studying the SWEETs in several plant species, especially *Arabidopsis* and rice, have contributed to a better understanding of SWEETs functional roles. There are few reports on the cloning and evolutionary analysis of *ZmSWEETs* [13,22,23]; however, no systematic and comprehensive studies were undertaken to characterize the *SWEET* genes and transporters of maize in relation to other cereal species, especially in the latest genome release. Therefore, considering the above knowledge gaps in the *SWEETs* family of maize and cereal systems, the present investigation was framed to mine and characterize the *SWEETs* in maize and related cereals to comprehensively understand the structural, evolutionary, regulatory, functional and genetic insights through in-depth comparative and functional analyses.

2. Materials and methods

2.1. Mining SWEET family sequences, physicochemical characterization, and chromosomal localization

The 17 Arabidopsis [10] and 21 rice [24] SWEET query sequences downloaded from TAIR (http://www.arabidopsis.org/) and RGAP (http://rice.uga.edu/) databases, respectively, were BLAST aligned (e-value <1e−5) with the *Zea mays* v5.0 proteome collected from the Ensemblplants database (https://plants.ensembl.org/) [25]. Additionally, the HMM (Hidden Markov Model) scanning of SWEET domain (PF03083) downloaded from the Pfam database (http://pfam.xfam. org/) was conducted in maize proteome with an *e-value* of 0.001. The resulting non-redundant protein sequences from BLASTp and HMM searches were examined for the presence of the SWEET domain using

SMART (http://smart.embl-heidelberg.de/) server. Subsequently, the gene models were named sequentially based on chromosomal positions. The ProtParam tool was employed to predict the physicochemical properties of each ZmSWEET protein [26].

2.2. Domain, motifs, and gene structure analysis of the SWEET family in maize

The SWEET domain features of ZmSWEET sequences were examined with Pfam and SMART databases with default parameters. The best ten conserved motifs in ZmSWEET proteins were predicted using the MEME server (https://meme-suite.org/meme/) with default parameters [27]. The GFF3 file of *Zea mays v5.0* was downloaded from the Ensemblplants database (https://plants.ensembl.org/) [25] to fetch the *ZmSWEET* gene structures. The domains, motifs and gene structure were visualized with TBtool [28].

2.3. Prediction of ZmSWEETs protein structures, active sites, and post-translational modifications

The secondary structure of ZmSWEET proteins was predicted through the SOPMA web server [29]. The three-dimensional (3D) structure of ZmSWEET proteins was predicted through the Phyre2 server [30] and evaluated with Ramachandran plot, ANOLEA (Atomic Non-Local Environment Assessment) and ProSA analyses. The CLICK server was employed to compare the ZmSWEET protein models through the RMSD value calculation based on α-carbon superposition [31]. The active sites of ZmSWEET proteins were predicted through CASTp 3.0 server [32].

2.4. Docking of ZmSWEET proteins with sugar molecules

The 3D structures of ligands viz., fructose ($C_6H_{12}O_6$; PubChem ID: 2723872), galactose ($C_6H_{12}O_6$; PubChem ID: 439357), glucose ($C_6H_{12}O_6$; PubChem ID: 5793) and sucrose ($C_{12}H_{22}O_{11}$; PubChem ID: 5988) were fetched from PubChem database (https://pubchem.ncbi. nlm.nih.gov/). The Autodock 4.2 and Autodock Vina software were employed to prepare the receptor proteins and ligands and docking simulations, respectively [33]. Subsequently, ZmSWEET-sugar interactions were analysed with PyMOL (https://pymol.org) and the LigPlot$^+$ v.2.2.4 software [34].

2.5. Multiple sequence alignment and phylogenetic analysis

The full-length SWEET protein sequences from maize and other Gramineae members, viz. rice, barley, sorghum, foxtail millet, pearl millet and *Brachypodium* were aligned through MUSCLE [35]. The phylogenetic analysis was performed with MEGAX software using the neighbor-joining (NJ) algorithm with 1000 bootstrap replicates and the Poison model as a replacement model [36].

2.6. Homology, collinearity, synteny and duplication analysis

OrthoFinder software [37] was used to study the homology among the *SWEET* families retrieved from barley, *Brachypodium*, foxtail millet, pearl millet, maize, rice and sorghum. The orthologous association among the *SWEET* members was visualized using Cytoscape software [38]. The whole proteome sequences of barley, *Brachypodium*, foxtail millet, maize, rice, and sorghum species were aligned with the BLASTp program (e-value <10^{-5}). Subsequently, the internal collinearity blocks of target proteomes were identified by implementing the MCScanX program [39]. The duplication pairs were identified based on coding sequence homology [40].

2.7. Selection pressure, divergence time and Ka/Ks analysis of SWEET members

The clustalW (https://www.genome.jp/tools-bin/clustalw) and ParaAT2.0 software were employed to align the sequences of *SWEET* ortholog pairs among the target cereal species. Subsequently, the aligned orthologues were used to calculate the nonsynonymous rate (Ka), synonymous rate (Ks), and evolutionary constraint (Ka/Ks) between each of the ortholog *SWEET* pairs using KaKs_calculator 3.0 with Nei-Gojobori method [41]. The neutral substitution rate of 1.5×10^{-8} per site per year was considered to estimate the divergence time between the SWEET orthologs [42].

2.8. Prediction of cis-acting elements and gene regulatory network analysis

The 2.0 kb upstream promoter region from the start codon of each *ZmSWEET* gene was scanned for *cis*-acting elements through the Plant-CARE database (http://bioinformatics.psb.ugent.be/webtools/plantcare/html/) [43]. The *ZmSWEET* regulatory elements, viz. transcription factors (TFs) and miRNAs were fetched from the PlantRegMap database [44] and psRNATarget tool [45], respectively. All the possible interactions among *ZmSWEETs* and regulatory elements, viz. *ZmSWEET*-TF, *ZmSWEET*-miRNA, miRNA-TF and TF-TF were predicted, and the network was realized with Cytoscape [38].

2.9. In silico expression and co-expression analyses of ZmSWEETs

The expression datasets across the growth phase and organs of the B73 genotype and kernel tissue of 40 maize inbred lines belonging to four maize sub-populations, viz. mixed (M), stalked-stiff (SS), non-stalked stiff (NSS) and tropical and subtropical (TSS) were retrieved from the Zeamap database [46]. To reveal the stress-responsive expression pattern of *ZmSWEETs,* the whole genome transcriptome data sets of abiotic stresses were collected for drought (NCBI Bio-projects: PRJNA782891; PRJNA545969), heat (NCBI Bio-project: PRJNA506720), salinity (NCBI Bio-project: PRJNA527733), and nitrogen starvation (NCBI Bio-project: PRJNA436973) (Table S1). The expression values of *ZmSWEETs* were retrieved from corresponding expressions datasets and calculated *log$_2$FC* values for uniform representation. The co-expression analysis of *ZmSWEET* genes was performed with ATTED-II (v.11.1) server [47] with the *coex* option on many genes and the PPI option on a few genes under maize.

2.10. Expression analysis of ZmSWEETs in maize germplasm showing variable tolerance to abiotic stresses

The seven maize inbred lines and three hybrids (Table S2) were grown in the controlled environment at the National Phytotron Facility, ICAR-IARI, New Delhi, in a randomized complete block design (RCBD) with three replications, and each replication carried three plants for control, drought, and waterlogging condition. The drought and waterlogging stresses were induced at a three-leaf stage and control sets were maintained under stress-free conditions [48–50] (Fig. S1). The primers for selected *ZmSWEET* genes were designed using primer3plus (https://primer3plus.com/cgi-bin/dev/primer3plus.cgi) web server with default parameters (Table S3).

The total RNA was isolated from the samples using the RNeasy kit (Qiagen, Hilden, Germany) as per the manufacturer's protocol. Using agarose gel electrophoresis and NanoDrop 1000 spectrophotometer, the quality and quantity of extracted RNA samples were analysed (Thermo Scientific, Wilmington, DE, USA). Subsequently, the mRNA samples showing good quality and quantity were converted into the first-strand complementary DNA (cDNA) using a cDNA-synthesis kit (Thermo Fisher Scientific, Waltham, MA, USA). The first-strand cDNA was investigated for expression using quantitative real-time polymerase chain reaction

(qRT-PCR) (Agilent Technologies, Santa Clara, CA. USA) with maize *ubiquitin* coding gene as an internal control. The PCR reactions were carried out at 95 °C for 4 min, followed by 40 cycles of 95 °C for 15 s, 60 °C for 30 s, and 72 °C for 1 min. The expression or CT values were analysed through the $2^{-\Delta\Delta CT}$ method [51].

2.11. Variable dominance of ZmSWEETs expression

The quantitative measurement of the F_1 expression level of each *ZmSWEET* gene related to an average of two parental lines (mid-parental level) was determined using a *d/a* ratio method [52,53]. Considering *d* as dominance, *a* as additive, and μ as the mid-parental value (average of the parental expression), the dominance (*d*) was measured as the difference between the F_1 (hybrid) and the average of the parents (μ) ($d = F_1 - \mu$). The additive effect (*a*) was measured by the difference between the parent (either maternal or paternal) and the average of the parents (μ) ($a = Parent - \mu$). In case of a complete dominant gene action of the P_1 (maternal) allele, $F_1 = P_1$, then $d/a = 1$. Similarly, $d/a = -1$ explains the complete dominant gene action of the P_2 (paternal) allelic expression. In the case of an additive gene action, $F_1 = \mu$, which is $d/a = 0$ [49].

3. Results

3.1. Mining of SWEET gene family sequences and physicochemical characterization

The genome-wide mining of SWEET genes in maize and related species through homology-based BLAST of rice and Arabidopsis SWEET query sequences and HMM search with SWEET domain PF03083 resulted in 20, 23, 22, 24, 21, 29 and 19 *SWEET* genes in maize (*ZmSWEETs*), sorghum (*SbSWEETs*), pearl millet (*CaSWEETs*), foxtail millet (*SiSWEETs*), rice (*OsSWEETs*), barley (*HvSWEETs*) and *Brachypodium* (*BdSWEETs*), respectively. The physicochemical properties of ZmSWEET proteins revealed wide variation in the protein length ranging from 208 (ZmSWEET7) to 401 (ZmSWEET1) amino acids with the corresponding molecular weight (MWs) of 22.66 and 43.26 kDa. The subcellular localization predictions showed that the majority of ZmSWEETs are localized in the plasma membrane (14), followed by the vacuolar membrane (4; ZmSWEET5, ZmSWEET7, ZmSWEET13, ZmSWEET15), chloroplast thylakoid membrane (2; ZmSWEET2, ZmSWEET18) and endoplasmic reticulum (1; ZmSWEET3). Most of the ZmSWEETs were found basic in nature (75 %) with an isoelectric point of *pI* > 7 whereas, ZmSWEET2, ZmSWEET5, ZmSWEET10, ZmSWEET12, and ZmSWEET14 were slightly acidic in nature with *pI* < 7. All the ZmSWEETs showed 7 TM domains except ZmSWEET18 (6TM) (Table 1; Table S4). The physicochemical properties of SWEET genes and proteins of related six species used for evolutionary analyses are summarized in Table S5. Further, the twenty *ZmSWEET* genes showed uneven distribution on maize chromosomes, with a maximum of five genes (*ZmSWEET4* to *ZmSWEET8*) on chromosome 3 to one gene each on chromosome 2 (*ZmSWEET3*), 6 (*ZmSWEET13*) and 9 (*ZmSWEET18*). However, *ZmSWEET* genes were not found on chromosome 7 (Fig. S2).

3.2. Structural analysis of SWEET genes and proteins in maize

3.2.1. Gene structure, protein motif and domains of SWEET members in maize

The gene structure analysis showed that the number of exons ranged from three (*ZmSWEET18*) to six (*ZmSWEET3, ZmSWEET5, ZmSWEET7, ZmSWEET9, ZmSWEET13 to ZmSWEET17*). Five exons were observed in *ZmSWEET1, ZmSWEET2, ZmSWEET4, ZmSWEET6, ZmSWEET19* and *ZmSWEET20* followed by four in *ZmSWEET8, ZmSWEET10, ZmSWEET11* and *ZmSWEET12*. Additionally, the majority of intronic sequences were found in phase 0 (66.02 %), followed by phase 1 (18.44 %) and 2 (15.53 %) (Fig. 1A; Table S6).

Table 1

The detailed descriptions of mined *ZmSWEETs* location and physicochemical properties of protein sequences.

Gene	Protein ID	Location				CDS Length	No. of TMD	Protein Length (aa)	*pI*	MW (kDa)	Localization
		Chromosome	Start (bp)	End (bp)	Strand						
ZmSWEET1	Zm00001eb016370_P002	1	57,388,423	57,391,530	+	1206	7	401	8.97	43.26	PM
ZmSWEET2	Zm00001eb016690_P001	1	59,332,122	59,335,202	−	921	7	306	6.82	33.39	CTM
ZmSWEET3	Zm00001eb113080_P002	2	229,238,918	229,241,758	+	1035	7	344	9.48	37.27	ER
ZmSWEET4	Zm00001eb119760_P001	3	3,007,579	3,009,415	+	915	7	304	9.45	32.77	PM
ZmSWEET5	Zm00001eb130550_P001	3	57,335,481	57,343,131	+	624	7	208	6.55	22.66	VM
ZmSWEET6	Zm00001eb133100_P002	3	95,886,707	95,888,621	+	888	7	295	9.64	32.28	PM
ZmSWEET7	Zm00001eb155660_P003	3	210,739,191	210,741,141	−	693	7	230	8.75	25.17	VM
ZmSWEET8	Zm00001eb161560_P002	3	229,383,794	229,386,907	+	705	7	234	9.03	26.23	PM
ZmSWEET9	Zm00001eb170150_P001	4	23,370,806	23,374,368	−	882	7	293	9.28	31.68	PM
ZmSWEET10	Zm00001eb180830_P001	4	99,858,093	99,859,991	+	915	7	304	5.67	32.94	PM
ZmSWEET11	Zm00001eb236820_P002	5	130,441,250	130,444,600	+	963	7	320	9.56	35.51	PM
ZmSWEET12	Zm00001eb241930_P002	5	168,139,385	168,142,816	+	1002	7	333	5.10	35.27	PM
ZmSWEET13	Zm00001eb288410_P002	6	159,025,680	159,028,453	−	753	7	250	8.90	26.77	VM
ZmSWEET14	Zm00001eb339850_P001	8	34,277,738	34,283,593	−	720	7	239	6.10	25.90	PM
ZmSWEET15	Zm00001eb342040_P001	8	60,365,663	60,368,090	−	732	7	243	8.71	26.60	VM
ZmSWEET16	Zm00001eb350590_P001	8	115,074,122	115,075,823	+	717	7	238	9.02	26.10	PM
ZmSWEET17	Zm00001eb357800_P002	8	145,653,930	145,656,997	+	732	7	243	8.87	26.91	PM
ZmSWEET18	Zm00001eb394800_P001	9	135,564,116	135,565,298	+	777	6	258	9.18	28.56	CTM
ZmSWEET19	Zm00001eb408900_P001	10	14,592,719	14,595,578	+	906	7	301	9.57	32.93	PM
ZmSWEET20	Zm00001eb408920_P001	10	14,827,732	14,830,329	+	909	7	302	9.57	32.95	PM

Note: aa, amino acid; CDS, coding sequence; CTM, chloroplast thylakoid membrane; ER, endoplasmic reticulum; Mw, molecular weight; pI: isoelectric point; PM, plasma membrane; TMD, transmembrane domain; VM, vacuole membrane.
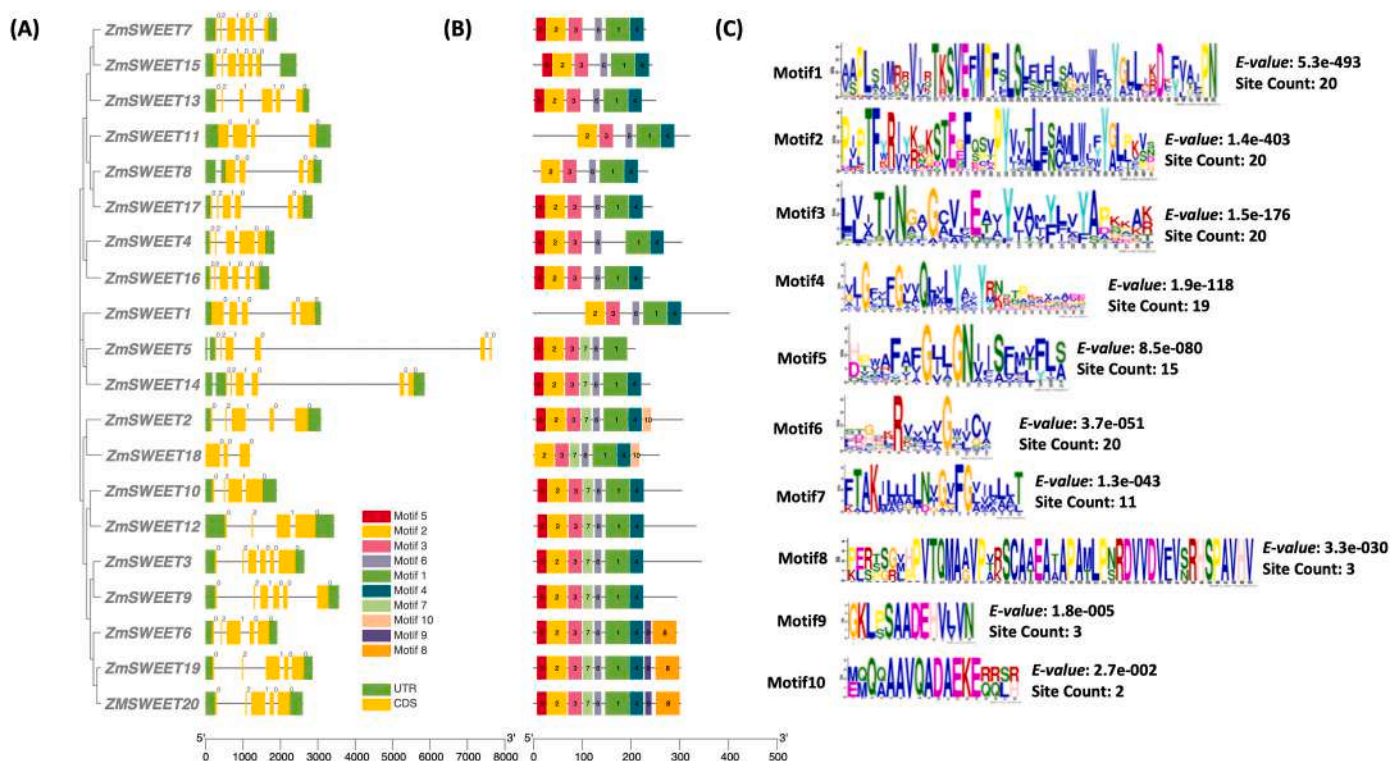

Fig. 1. The phylogenetic relationship, gene structure and distribution of conserved motifs of *ZmSWEET* genes and protein sequences: (A) The gene architectures of *ZmSWEET* genes depicting the distribution of exons and introns. The line denotes intron sequences, the yellow box denotes the exons and the green box denotes untranslated regions. (B) Distribution of conserved motifs in the ZmSWEET proteins. Each motif is depicted in a different colour. (C) The logo and site counts of statistically significant motifs identified in the ZmSWEET proteins.

A motif is a consensus or conserved region of protein or nucleotide sequences mediating the regulatory functions of genes or proteins through transcriptional and post-translational interactions. The MEME server identified ten conserved motifs distributed among 20 ZmSWEET proteins (Fig. 1B; C). Motifs 1, 2, 3 and 6 were present in all the 20 ZmSWEETs. The next widely distributed motif was 5 among 16 ZmSWEETs except for ZmSWEET1, ZmSWEET8, ZmSWEET11, and

ZmSWEET18. The transmembrane domain analysis showed that except ZmSWEET18 (6TM) all the ZmSWEETs showed 7 TMs, which are distributed throughout the ZmSWEET proteins (Table S7).

3.2.2. Prediction of ZmSWEET proteins structures and post-translational modifications

Total phosphorylation sites on ZmSWEET proteins varied from 12

(ZmSWEET5) to 42 (ZmSWEET1). The maximum phosphorylation sites were predicted on serine (257), followed by threonine (128) and tyrosine (53) (Fig. S3). The N- and O- glycosylations were exhibited by 60 % and 30 % of ZmSWEETs, respectively. The ZmSWEETs, viz., ZmSWEET6, ZmSWEET9, ZmSWEET16, ZmSWEET17, and ZmSWEET19 showed both N- and O- glycosylations whereas, no glycosylations sites were identified in ZmSWEET2, ZmSWEET4, ZmSWEET5, ZmSWEET12, ZmSWEET13, ZmSWEET14 and ZmSWEET18 (Fig. S4).

The ZmSWEETs predominantly showed alpha-helices (62–88 %) followed by TM helix (37–71 %), disordered region (5–33 %), and betasheets (0–6 %) (Table S8). The predominance of alpha helices facilitates the formation of hydrogen bonds to make the protein structure more stable. The TM helices were lowest in ZmSWEET1 (37 %) and highest in ZmSWEET5 (71 %). The lowest disordered regions were predicted in ZmSWEET5 (5 %) and the highest in ZmSWEET12 (33 %). In contrast to alpha helices, TM domains and disordered regions, the beta sheets were identified only in 50 % of ZmSWEETs with the highest percentage in ZmSWEET1 and ZmSWEET11 (6 %). Whereas, ZmSWEET3, ZmSWEET5-ZmSWEET9, ZmSWEET14, ZmSWEET15, ZmSWEET16 and ZmSWEET20 were devoid of beta sheets (Table S8). The alignment of ZmSWEETs-templates in 3D models showed confidence interval of 100 % with a coverage of 57 % (ZmSWEET1) to 99 % (ZmSWEET5) (Fig. 2).

Ramachandran plot analysis of ZmSWEET 3D structures showed that ZmSWEET1, ZmSWEET2, ZmSWEET6, ZmSWEET11, ZmSWEET13, ZmSWEET17, ZmSWEET18 and ZmSWEET19 were having 0 % and > 98 % of residues distribution in disallowed and most favoured regions, respectively. However, the rest of the 12 ZmSWEETs showed >96 % of residues in the most favoured regions; the residues in disallowed regions vary from 0.41 to 1.08 % (Fig. S5; Table S9). The ProSA z-scores of ZmSWEET structures ranged from −4.79 (ZmSWEET7) to −1.18 (ZmSWEET16), typically plotted within the range of scores for native proteins of similar size from X-ray crystallography and NMR sources, suggesting no significant deviation from the native structures. Furthermore, the ANOLEA z-scores ranged from 4.76 (ZmSWEET6) to 10.6 (ZmSWEET8) (Table S9). The RMSD values for all the pairs showed <2 Å and similarity percentages from 80.66 to 100 % (Table S10).

3.2.3. Molecular docking of SWEET proteins in maize

Four sugar molecules, viz. fructose ($C_6H_{12}O_6$; PubChem ID: 2723872), galactose ($C_6H_{12}O_6$; PubChem ID: 439357), glucose ($C_6H_{12}O_6$; PubChem ID: 5793) and sucrose ($C_{12}H_{22}O_{11}$; PubChem ID: 5988) were used as ligands in molecular docking with ZmSWEETs. Relatively, ZmSWEETs showed the lowest mean binding energy (ΔG) and predicted inhibition constant (*pki*) for sucrose (ΔG: −6.22 kcal/mol; *pki*: 64.70 μmol) compared to fructose (ΔG: −5.03 kcal/mol; *pki*: 285.64 μmol), galactose (ΔG: −5.18 kcal/mol; pki: 229.05 μmol) and glucose (ΔG: −5.37 kcal/mol; pki: 191.69 μmol). Among all the ZmSWEETs, the ZmSWEET14 showed the lowest ΔG and *pki* with fructose (ΔG: −6.20 kcal/mol; pki: 28.20 μmol), galactose (ΔG: −6.00 kcal/mol; *pki*: 39.54 μmol) and glucose (ΔG: −6.10 kcal/mol; *pki*: 33.40 μmol); whereas, ZmSWEET17 showed the lowest ΔG and *pki* with glucose (ΔG: −6.10 kcal/mol; *pki*: 33.40 μmol) and sucrose (ΔG: −7.50 kcal/mol; *pki*: 3.14 μmol) (Table 2; Fig. 3).

The hydrogen interactions were varied from 2 to 7 in ZmSWEETsfructose and ZmSWEET-galactose interactions. The ZmSWEET14 with the lowest ΔG showed six hydrogen bonds with fructose through three asparagine residues (Asn71, Asn139, Asn193) and hydrophobic interactions via four amino acid residues (val70, Trp54, Asn173, Trp177). Similarly, in the case of ZmSWEET-galactose, ZmSWEET14 showed two hydrogen bonds with Asn139 and Asn193 and hydrophobic interactions with Trp54, val70, Asn71, Trp177 and leu189 (Fig. 3; Table S11; Fig. S6-S9).

The docking of ZmSWEETs with glucose showed three (ZmsWEET16) to eight (ZmSWEET1) hydrogen bonds. In ZmSWEET-glucose docking, four hydrogen bonds were observed in the proteins showing the lowest ΔG, viz. ZmSWEET17 (Asn76, Tyr146, Asn196)

(Fig. 3) and ZmSWEET16 (Asn71, Asn139, Asn193). Further, Val and Trp residues were common in the hydrophobic interactions. The ZmSWEET-sucrose docking revealed the hydrogen bonds varying from 4 (ZmSWEET9, ZmSWEET14 and ZmSWEET15) to 9 (ZmSWEET1). The protein ZmSWEET17 with the highest binding affinity showed six hydrogen bonds with Asn76, Tyr146, Ser173, Gly199 and Asn196 residues and hydrophobic interactions with Asn53, Trp57, Gly142, Gly177, Asn176 and Trp180 (Fig. 3). Interestingly, asparagine showed the most frequent appearance in establishing hydrogen bonds between sugars and ZmSWEET proteins (Table S11; Fig. S6-S9).

3.3. Evolutionary genetics of SWEETs in maize and Poaceae species

3.3.1. Phylogenetic analysis of SWEET family

The topology of the phylogenetic tree classified 158 SWEET proteins into eight groups named I to VIII. Groups I and IV emerged as the largest groups with 45 SWEET transporters, followed by group VI with 17 SWEET transporters. Group II, III, V, VI, VII and VIII showed 8, 14, 8, 17, 15 and 6 SWEET transporters, respectively, with at least one SWEET member from each target taxa. Group VII clustered the maximum number of OsSWEETs ($N=6$). Further, group VI clustered three copies of SWEET transporters each from sorghum, foxtail millet and pearl millet. Group VIII emerged as the smallest group with six SWEET transporters, each belonging to all six species except maize. Overall, the phylogeny showed a mixed grouping pattern of SWEETs rather than crop-specific grouping (Fig. 4).

3.3.2. Duplication of SWEET genes in maize

The duplication analysis of *ZmSWEET* genes was performed to examine the SWEET genes expansion within the maize genome. The duplication analysis revealed 14 duplication pairs among 13 *ZmSWEET* genes with a minimum of 80 % identity and 500 bp alignment length (Fig. S10). The 14 pairs of *ZmSWEET* duplicates were found distributed on eight chromosomes. Among the detected duplication pairs, *ZmSWEET2, ZmSWEET5, ZmSWEET8* and *ZmSWEET10* genes showed one-to-one duplications with *ZmSWEET18, ZmSWEET14, ZmSWEET17* and *ZmSWEET12,* respectively. However, ZmSWEET3*, ZmSWEET6, ZmSWEET9, ZmSWEET19* and *ZmSWEET20* showed many-to many duplications among each other. The selection pressure and divergence time analyses showed a mean Ka/Ks ratio of 0.36 with a range of 0.17 (*ZmSWEET8-ZmSWEET17*) to 0.58 (*ZmSWEET10-ZmSWEET12*), suggesting the evolution of *ZmSWEET* duplications under strong purifying selection between 9.47 and 48.39 MYA (Table S12).

3.3.3. Synteny and orthology of SWEETs in Poaceae lineage

The pairwise syntenic associations among the seven target species were used to dissect the synteny among *SWEET* genes (Table 3; Fig. S11-S12). The maximum collinear blocks with SWEET genes were observed in sorghum-foxtail millet (20), followed by pearl millet-sorghum (16), foxtail millet-rice (16), rice-sorghum (16), and *Brachypodium*-foxtail millet (15). Similarly, the maximum SWEET gene pairs in collinear blocks were observed between foxtail millet-sorghum (22) followed by rice-sorghum (19), foxtail millet-rice (18), and *Brachypodium*-foxtail millet (17). Interestingly, no significant association was reported between the total number of collinear blocks with SWEET genes ($r = −0.36^{NS}$). On the contrary, a significant and positive correlation was observed between percentage of the total genes in collinear blocks of the genomes and the percentage of collinear SWEET genes of species-1 ($r = 0.75^{**}$) and species-2 ($r = 0.65^{**}$). Furthermore, a weak and nonsignificant association was observed between the number of total genes and a total number of SWEET genes from both the syntenic species ($r = −0.17^{NS}$) (Fig. S13).

The *ZmSWEET* genes showed the maximum syntenic relationship (65 %) with sorghum (43.48 %) and foxtail millet (45.83 %) SWEET genes. However, the lowest synteny was observed between maize (5 %) and barley (6.90 %). Further, the syntenic blocks from nine
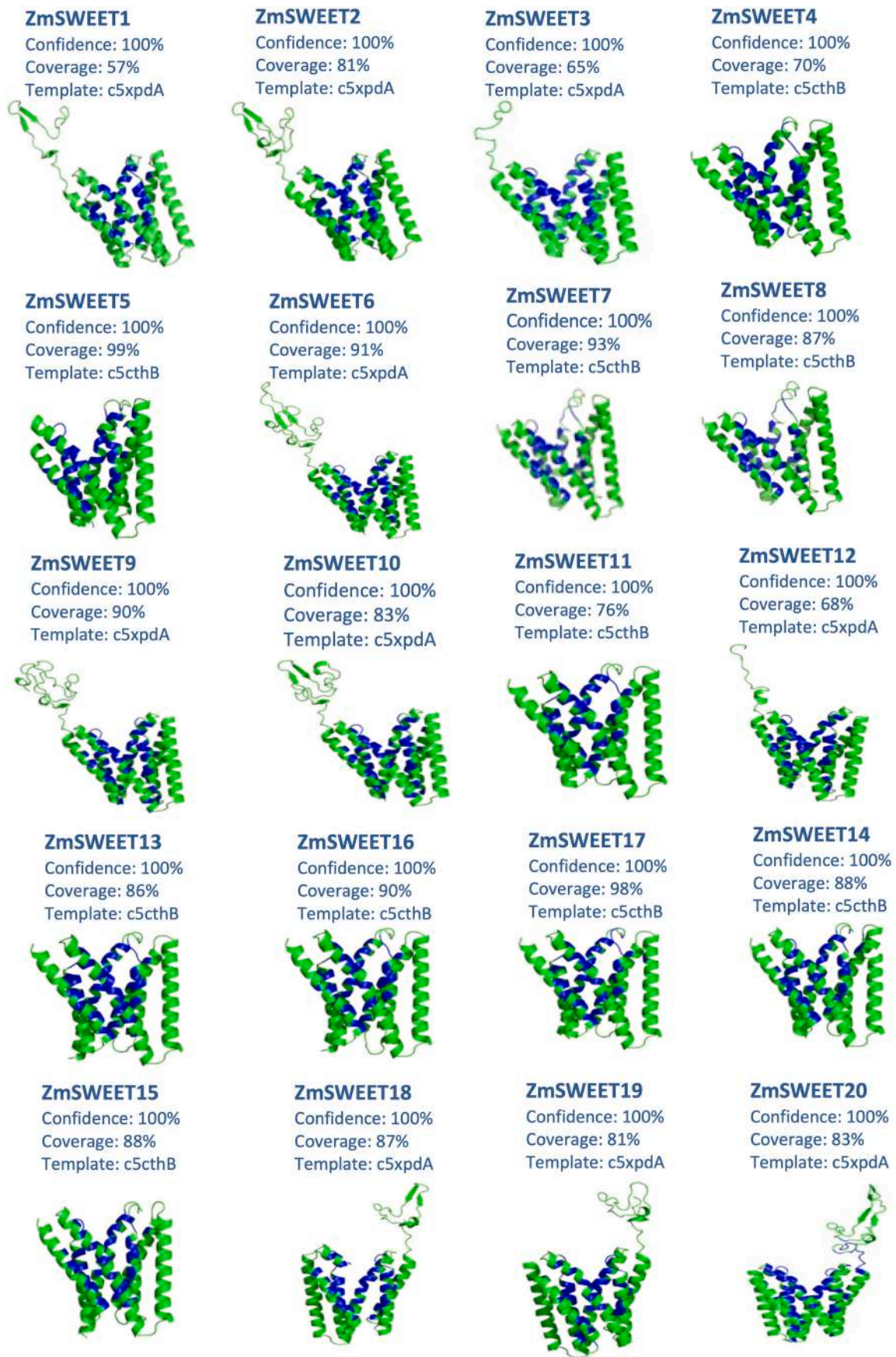
Fig. 2. The three-dimensional structure of ZmSWEET proteins: Each protein structure is accompanied with a percentage of confidence score and coverage with the best template used for building of 3D models.

Table 2

The results of ZmSWEET-sugar docking analyses showing the binding energies, inhibition constants and number of hydrogen bonds formed in each ZmSWEET-sugar interaction.

S. No.	Protein	Theor. Weight (kDa)	Sugar (Ligand)											
			Fructose			Galactose			Glucose			Sucrose		
			ΔG (kcal/mol)	pKi (μmol)	#H-bonds	ΔG (kcal/mol)	pKi (μmol)	#H-bonds	ΔG (kcal/mol)	pKi (μmol)	#H-bonds	ΔG (kcal/mol)	pKi (μmol)	#H-bonds
1	ZmSWEET1	43.26	−5.40	108.99	4	−5.70	65.65	5	−6.00	39.54	8	−7.10	6.16	9
2	ZmSWEET2	33.39	−4.70	355.67	6	−4.70	355.67	4	−5.50	92.04	4	−6.50	16.99	8
3	ZmSWEET3	37.27	−4.90	253.68	5	−5.10	180.94	7	−5.70	65.65	7	−6.50	16.99	5
4	ZmSWEET4	32.78	−4.50	498.67	4	−5.60	77.73	7	−5.60	77.73	8	−7.00	7.30	6
5	ZmSWEET5	22.67	−6.10	33.40	6	−4.20	827.87	4	−4.20	827.87	6	−5.30	129.05	6
6	ZmSWEET6	32.28	−5.00	214.24	7	−5.30	129.05	7	−5.60	77.73	5	−6.50	16.99	6
7	ZmSWEET7	25.17	−4.80	300.38	7	−4.30	699.16	4	−4.40	590.47	5	−5.40	108.99	8
8	ZmSWEET8	26.23	−5.60	77.73	2	−5.50	92.04	2	−5.80	55.44	4	−5.60	77.73	7
9	ZmSWEET9	31.68	−4.90	253.68	5	−5.30	129.05	7	−5.60	77.73	6	−4.60	421.15	4
10	ZmSWEET10	32.94	−4.90	253.68	5	−5.30	129.05	7	−5.60	77.73	4	−6.50	16.99	5
11	ZmSWEET11	35.51	−5.60	77.73	2	−5.50	92.04	2	−5.90	46.82	4	−5.40	108.99	9
12	ZmSWEET12	35.27	−4.20	827.87	3	−5.10	180.94	7	−5.60	77.73	6	−6.40	20.12	6
13	ZmSWEET13	26.77	−4.40	590.47	5	−5.20	152.81	7	−5.30	129.05	6	−5.30	129.05	6
14	ZmSWEET14	25.91	−6.20	28.20	6	−6.00	39.54	2	−6.10	33.40	4	−7.30	4.40	4
15	ZmSWEET15	26.61	−4.90	253.68	7	−4.30	699.16	5	−4.60	421.15	6	−5.30	129.05	4
16	ZmSWEET16	26.10	−4.30	699.16	2	−5.20	152.81	2	−4.40	590.47	3	−7.30	4.40	8
17	ZmSWEET17	26.91	−5.60	77.73	3	−5.70	65.65	4	−6.10	33.40	4	−7.50	3.14	6
18	ZmSWEET18	28.56	−4.80	300.38	6	−4.90	253.68	6	−5.20	152.81	4	−6.20	28.20	6
19	ZmSWEET19	32.93	−4.90	253.68	5	−5.30	129.05	7	−5.20	152.81	5	−6.20	28.20	6
20	ZmSWEET20	32.95	−4.90	253.68	5	−5.30	129.05	7	−5.00	214.24	5	−6.40	20.12	7

Note: ΔG, binding energy (kcal/mol); *pKi,* predicted inhibition constant (μmol); #H-bonds, number of hydrogen bonds between ZmSWEET proteins and corresponding sugar ligands.

chromosomes of maize (except 7) showed collinearity for SWEET genes with *Brachypodium,* foxtail millet, and sorghum. Whereas rice, pearl millet and barley shared SWEET collinearity with the chromosome 8, 7 and 2 of maize. Interestingly, barley showed the lowest syntenic collinear blocks of sweet genes with all other six species.

Based on homology, OrthoFinder grouped 158 SWEET sequences into 14 orthologous groups (OG). The OG00 showed the highest number of orthologous SWEET pairs (246), followed by OG01 (104) and OG03 (88)) (Fig. S14). It was shown that the gene family size in a species is not always correlated with the divergence of gene family members [54]. The commonality of OGs from 50 to 100 % was observed among the target cereals. The *Brachypodium,* followed by pearl millet, shared the maximum OGs with the remaining species under investigation. The rice, sorghum, foxtail millet and maize share 100 % of their OGs with *Brachypodium.* Similarly, rice, sorghum and foxtail millet shared 100 % orthologous groups with pearl millet. Interestingly, all the OGs were found to be common between sorghum and foxtail millet. However, the barley and maize recorded a minimal share of OGs with other target species (Fig. 5).

The 100 % ZmSWEETs were found orthologous with 82.60 % of sorghum and 70.83 % of foxtail millet. Among all the pairwise comparisons of SWEET repertoires, *CaSWEETs* showed the lowest orthologous percentages, viz. 55.17 %, 68.96 % and 72.41 %, with maize (80 %), pearl millet (72.27 %) and rice (80.95 %), correspondingly (Fig. 5). Therefore, orthologous homology among the cereal *SWEET* sequences suggested that *HvSWEETs* showed appreciable divergence than the remaining *SWEET* sequences whereas, *ZmSWEETs* sequences are highly conserved with *SbSWEET* and *SiSWEET* sequences.

3.3.4. Selection pressure and divergence period of SWEET orthologs

The Ka/Ks ratio with statistical significance ($p < 0.05$) was obtained for 486 orthologous *SWEET* gene pairs from the target Poaceae species. All the SWEET orthologs except *BdSWEET5-SbSWEET13* (Ka/Ks = 1.52; $p < 0.01$) showed Ka/Ks values <1.0, indicating the selective purifying selection during the evolution and divergence of *SWEET* genes (Table 4; Table S13). A wider range of divergence periods was observed between *OsSWEETs* and *HvSWEETs* (19.12–81.42 MYA) and foxtail millet and

maize (14.75–73.31 MYA). However, the mean divergence period was highest between *OsSWEETs* and *SbSWEETs* (44.58 MYA) and *ZmSWEETs* and *HvSWEETs* (43.56 MYA) (Table 4).

3.4. Functional, regulatory and genetic analysis of SWEET genes in maize

3.4.1. Analysis of cis-acting elements of SWEET genes in maize

The *cis*-acting elements retrieved from 2 kb upstream sequences of *ZmSWEETs* were grouped under five categories, viz. core promoter elements (CPE), hormone, light, stress-responsive and growth and development-related elements (Fig. 6; Table S14). Promoter sequences of all the *ZmSWEET* genes showed a high occurrence of core elements viz., *AT ~ TATA-box*, *CAAT-box* and *TATA-box*, except *ZmSWEET15,* which lacks *AT ~ TATA-box* element (Table S14; Fig. S15). Among growth and development-related *cis*-acting elements (GDE), *CAT*-box regulating meristem growth, *RY* element associated with seed-specific expression and *O₂-site* involved in the regulation of zein metabolism in maize were found in >50 % of *ZmSWEET* genes (Table S14; Fig. S16). A total of 247 light responsiveness *cis*-acting elements (LRE) belonging to 25 kinds were identified. The maximum number of LREs (20) were distributed in the promoter sequences of *ZmSWEET9, ZmSWEET10* and *ZmSWEET12.* The *G-box* (84), followed by *GT1-motif* (27), *Box-4* (26) and *TCCC-motif* (15) are the most prominent LREs fund in *ZmSWEETs* (Table S14; Fig. S17). Further, 176 copies of 10 hormone-responsive *cis*-acting elements (HRE) were classified into gibberellin (*CARE, GARE, P-box,* and *TATC-box*), auxin (*AuxRR-core, TGA*), salicylic acid (*TCA*), ethylene (*ERE*) and methyl jasmonate (*CGTCA-motif, TGACG-motif*) responsive elements. Both *CGTCA-motif* (55) and *TGACG-motif* (55) elements were present in maximum number and distributed across all the *SWEET* genes except *ZmSWEET5, ZmSWEET6, ZmSWEET14* and *ZmSWEET19* (Table S14; Fig. S18).

With 655 copies of stress-responsive *cis*-acting elements (SRE) falling under 33 kinds was emerged as one of the major categories in *ZmSWEET* promoters. Among these, typical drought-responsive (*MYC:* 89; *MYB* 73) and osmotic stress-associated (*ABRE:* 84) elements were found prominent. The 262 MYB transcription factor recognition and binding site elements (*MBS, MBSL, MYB, MYB-recognition site, MYB-binding site,*
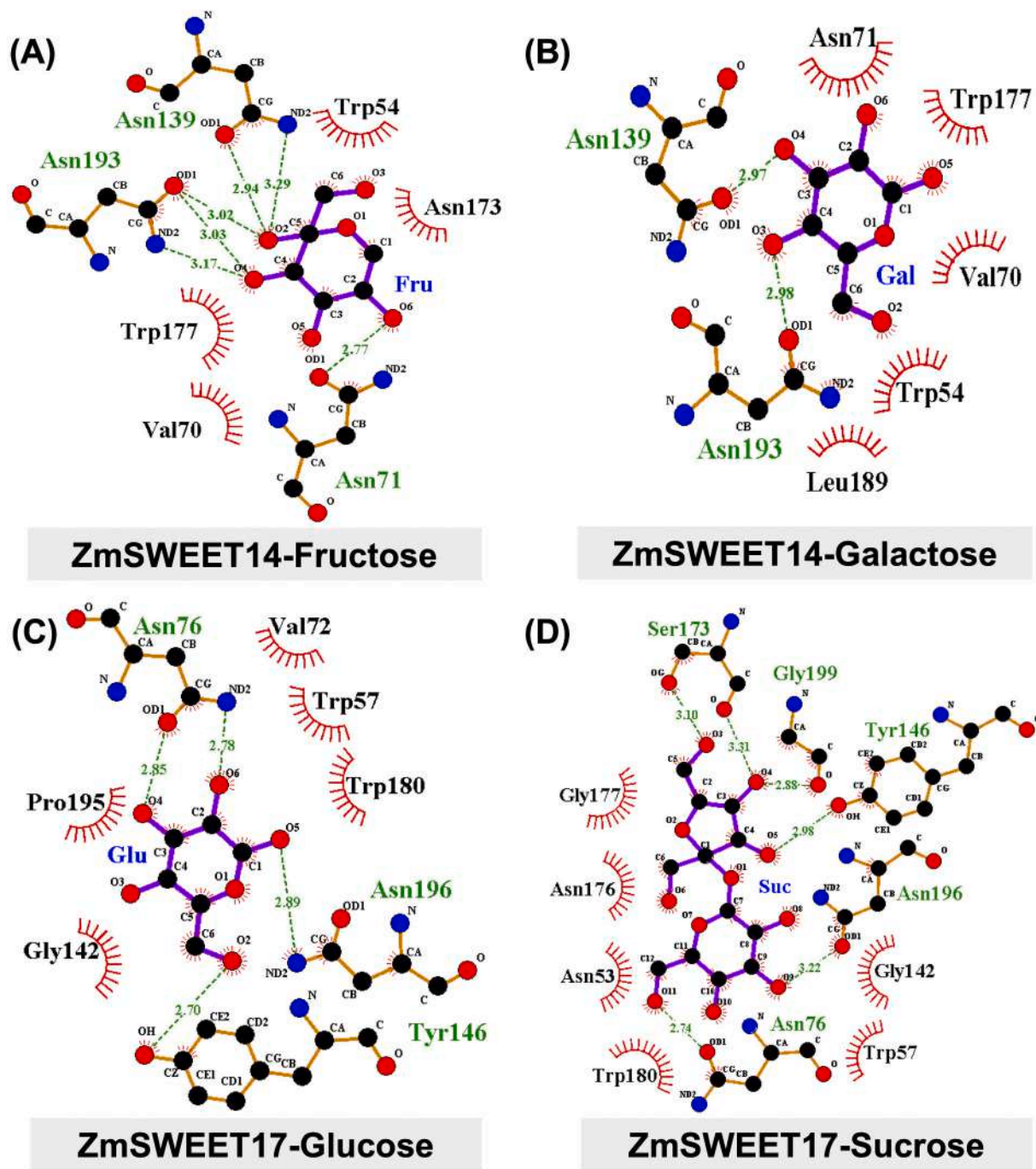
Fig. 3. The molecular docking of ZmSWEET-sugar interactions: The ZmSWEET transporters showing lowest binding energy and inhibition constant with four sugar ligands: (A) ZmSWEET14-fructose, (B) ZmSWEET14-galactose, (C) ZmSWEET17-glucose, and ZmSWEET17-sucrose. For remaining SWEET-sugars interactions please see Figs. S7–S10.

MYB-like sequence and *MYC*) were distributed among the promoters of *ZmSWEETs*. Additionally, *ARE* (anaerobic responsive element) was present in the promoter sequence of 14 *ZmSWEET* genes and waterlogging-responsive element (*C-box*) in *ZmSWEET13*. Other important SRE included *AT-rich sequence, LTR* (low-temperature responsive element), *WUN*-motif (wound-responsive element) etc. (Table S14; Fig. S19).

3.4.2. In silico expression of ZmSWEET genes in tissues and diverse genotypic sets

The maize expression dataset across 23 different tissues of B73 (a classical maize cultivar) and kernel tissues of 40 maize inbred lines

belonging to diverse sub-population bases, viz. non-stiff-stalk (NSS), stiff-stalk (SS), tropical and sub-tropical (TST) and mixed (M) populations were retrieved from Zeamap database (http://www.zeamap. com/; 7 July 2022). Except for *ZmSWEET18*, B73 showed variable expression of *ZmSWEETs* in various tissues. A higher expression of *ZmSWEET14* was observed in the root tissues (FPKM: 53.69-394.04). Internodal stages (6–7: 35.97; 7–8: 25.52) and reproductive tissues like ear primordium (2–4 mm: 99.25; 6-8 mm: 64.67) and embryo (20 DAP: 179.36; 38 DAP: 43.10) showed moderately higher expression of *ZmSWEETs*. Interestingly, the endosperm showed very low (12DAP: 1.19) and Nil (38 DAP: 0.00) expressions of *ZmSWEET11* whereas, the higher expressions were observed in the embryo (Fig. 7A). Among all the
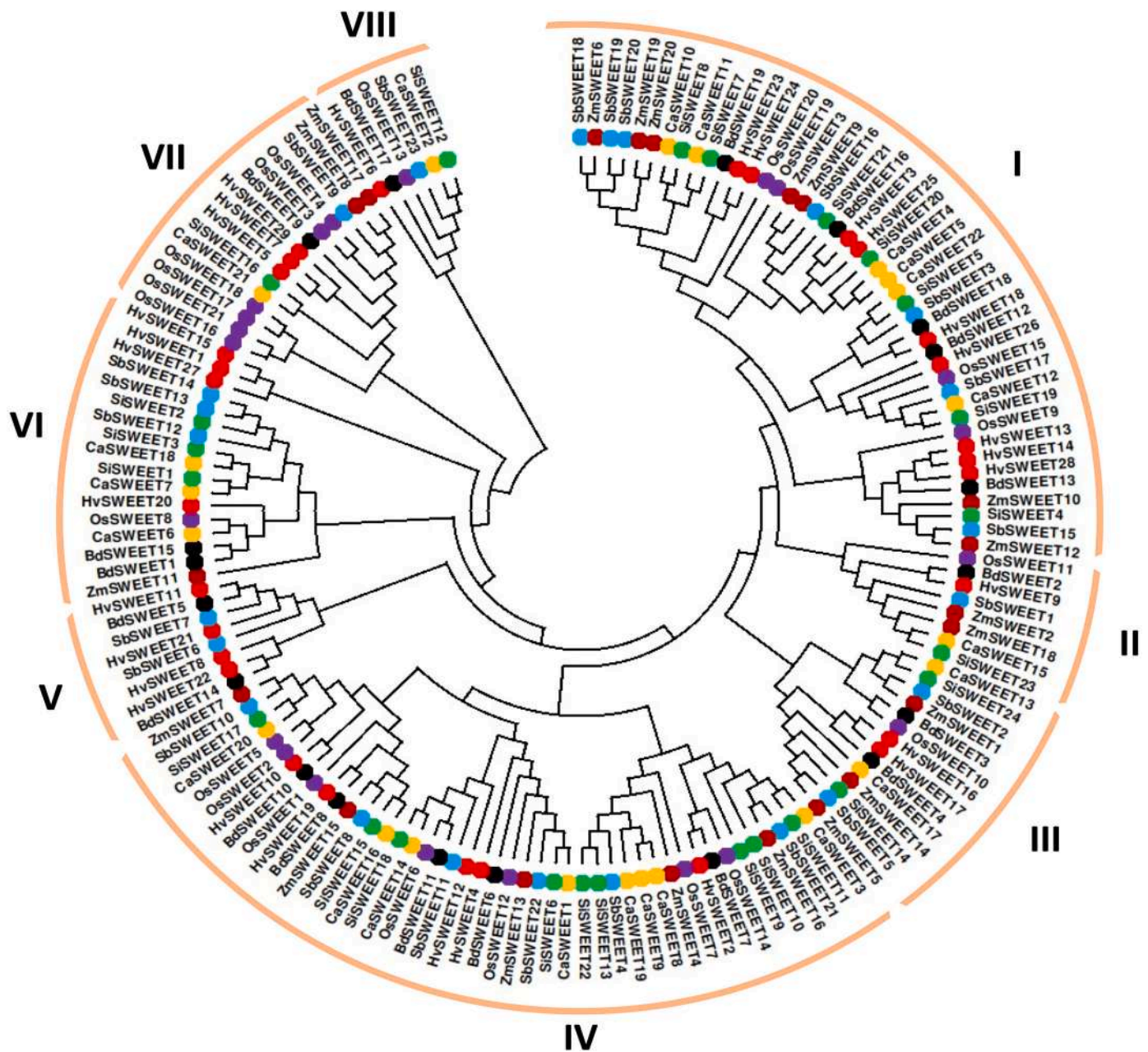
Fig. 4. The phylogenetics of SWEET transporters in cereals: The phylogenetic relationship of 158 SWEET transporters from maize and related species. The phylogenetic tree topology was generated through MEGA11 with neighbor-joining method and 1000 bootstrap replications. Branches corresponding to partitions reproduced in <50 % bootstrap replicates are collapsed.. The evolutionary distance matrices were computed using the JTT matrix-based method.

ZmSWEET genes, *ZmSWEET15* showed expression across 23 tissues (FPKM: 1.20-16.54), followed by *ZmSWEET11* (FPKM: 1.19-179.36) in 20 tissues. Further, the female spikelet, germinating kernels, primary and secondary roots showed the highest number (14) of *ZmSWEETs* expression, among which *ZmSWEET1, ZmSWEET6, ZmSWEET7, ZmSWEET9-ZmSWEET11, ZmSWEET15, ZmSWEET19* and *ZmSWEET20* were found common (Fig. 7A). Further, ZmSWEET*11* and *ZmSWEET12* showed higher expression in the kernel tissues of 40 diverse inbred lines of four sub-populations and B73 (Fig. 7A-E). Similarly, *ZmSWEET1, ZmSWEET3, ZmSWEET8, ZmSWEET10, ZmSWEET11, ZmSWEET13* and *ZmSWEET15* showed expression across the lines and subpopulations. However, *ZmSWEET2, ZmSWEET4-ZmSWEET6,* and *ZmSWEET16-ZmSWEET18* showed inconsistent expression among the sub-populations and inbreds. Therefore, the genetic background exhibits significant interactions and influences *ZmSWEETs* expression (Fig. 7B-E).

3.4.3. In silico expression analysis of ZmSWEET genes under abiotic stresses

Drought stress resulted in enhanced expression of *ZmSWEETs* in the leaf tissues of Xianyu335 (*ZmSWEET2*: 1.03, *ZmSWEET11:* 1.48, *ZmSWEET13*: 1.12) and B104 (*ZmSWEET8:* 3.07, *ZmSWEET5:* 1.53, *ZmSWEET11:* 4.87) genotypes. Interestingly, *ZmSWEET15* showed enhanced expression in leaves of both Xianyu335 (2.04) and B104 (1.74) genotypes. Further, *ZmSWEET8* and *ZmSWEET15* showed increased expression in leaves, ear (*ZmSWEET8*: 1.13; *ZmSWEET15*: 1.13) and kernels (*ZmSWEET8*: 2.03; *ZmSWEET15*: 1.29) of B104 genotype. The ZmSWEET19 showed enhanced expression in both the reproductive tissues of B104 (ear: 1.10; kernel: 1.07) whereas, decreased expression was observed in leaves (−2.60) (Fig. 8).

Table 3

The genome-wide and SWEET genes specific synteny and collinearity blocks among *Brachypodium*, barley, foxtail millet, maize, pear millet, rice and sorghum.

Syntenic Pair (S1–S2)	All genes				SWEET genes							
	Total CB	Genes in CB	Total genes	Percentage (%)	No. of CB	Gene pairs in CB	No. of genes S1	No. of genes S2	Total genes S1	Total genes S2	Percentage (S1)	Percentage (S2)
Maize-Barley	757	28,046	75,583	37.11	2	2	1	2	20	29	5.00	6.90
Maize-Brachypodium	835	34,878	72,195	48.31	14	13	12	9	20	19	60.00	47.37
Maize-Foxtail millet	797	38,836	74,340	52.24	15	15	13	11	20	24	65.00	45.83
Maize-Pearl millet	920	30,114	78,335	38.44	9	9	9	6	20	22	45.00	27.27
Maize-Rice	776	35,554	81,945	43.39	12	12	10	10	20	21	50.00	47.62
Maize-Sorghum	681	41,605	73,885	56.31	14	14	13	10	20	23	65.00	43.48
Brachypodium-Barley	541	28,752	68,266	42.12	8	8	6	6	19	29	31.58	20.69
Brachypodium-Foxtail millet	596	34,768	67,023	51.87	15	17	12	13	19	24	63.16	54.17
Brachypodium-Pearl millet	669	26,250	71,018	36.96	13	13	11	10	19	22	57.89	45.45
Brachypodium-Rice	540	34,278	74,628	45.93	11	14	11	11	19	21	57.89	52.38
Brachypodium-Sorghum	477	33,087	66,568	49.70	14	17	12	13	19	23	63.16	56.52
Foxtail millet-Barley	534	27,675	70,411	39.30	6	6	4	4	24	29	12.50	10.34
Foxtail millet-Pearl millet	760	34,427	73,163	47.06	13	13	11	10	24	22	45.83	45.45
Foxtail millet-Rice	527	36,421	76,773	47.44	16	18	14	12	24	21	58.33	57.14
Foxtail millet-Sorghum	440	38,265	68,713	55.69	20	22	16	15	24	23	66.67	65.22
Pearl millet-Barley	556	21,070	74,406	28.32	5	5	3	3	22	29	13.64	10.34
Pearl millet-Rice	684	27,839	80,768	34.47	12	12	11	11	22	21	50.00	52.38
Pearl millet-Sorghum	664	30,215	72,708	41.56	16	16	13	14	22	23	59.09	60.87
Rice-Barley	501	27,492	78,016	35.24	4	4	3	4	21	29	14.29	13.79
Rice-Sorghum	414	34,391	76,318	45.06	16	19	14	14	21	23	66.67	60.87
Sorghum-Barley	461	26,695	69,956	38.16	6	6	6	4	23	29	26.09	13.79

Note: CB, collinear block; S1, species 1; S2, species 2.

Under heat stress, the genes *ZmSWEET8* (Annong591: 5.81; CB25: 5.76; CB1: 6.35), *ZmSWEET6* (Annong591: 1.18; CB25: 1.63; CB1: 1.98), and *ZmSWEET16* (Annong591: 1.98; CB25: 2.40; CB1: 2.07) showed enhanced expression in the leaves of parental lines and hybrid. Whereas, *ZmSWEET5* (Annong591: -1.19; CB25: -2.41; CB25: −3.05) and *ZmSWEET719* (Annong591: -2.96; CB25: -2.08; CB1: −3.08) showed decreased expression. More number of *ZmSWEET* genes showed increased expression in roots of salinity-tolerant genotype ST (*ZmSWEET3*: 2.68; *ZmSWEET6*: 1.59; *ZmSWEET10*: 1.01; *ZmSWEET11*: 1.12; *ZmSWEET13*: 2.30) as compared to sensitive genotype SS (*ZmSWEET2*: 4.11; *ZmSWEET8*: 4.06) under salt stress. However, ZmSWEET1 showed increased expression in the roots of both genotypes (SS: 1.65; ST: 2.68). Contrary to the above stresses, nitrogen starvation showed decreased expression of *ZmSWEETs* in the leaves of the B73 genotype. The *ZmSWEET10* and *ZmSWEET20* showed decreased expression in both leaf differentiation (*ZmSWEET10*: −4.39; *ZmSWEET20*: −3.05) and elongation (*ZmSWEET10*: −1.58; *ZmSWEET20*: −2.02) zones.

3.4.4. Expression and variable dominance of ZmSWEET genes in maize under abiotic stresses

The expression of *ZmSWEET3, ZmSWEET7, ZmSWEET9, ZmSWEET10* and *ZmSWEET11* genes were recorded in the shoot and root of seven diverse maize inbreds and three experimental hybrids under drought and waterlogging stresses (Fig. 9). The stress-sensitive maize inbred line PML10 showed downregulation and non-significant expression (< *1log2fold*) of all the five target genes under drought and waterlogging stresses in root and shoot tissues except an enhanced expression of *ZmSWEET10* in shoot under waterlogging stress (5.39). On the other hand, PML93 mostly showed enhanced expression of five genes under drought and waterlogging stresses (1.28 to 6.62) (Fig. 9). Further, all five genes showed enhanced expression in response to target stresses in the LM13 × CML563 hybrid whereas, PML69 × CML563 showed increased expression of *ZmSWEETs* in root tissue under waterlogging stress only (0.93 to 6.12). The genes *ZmSWEET9* (drought: −3.11; waterlogging: −3.88), *ZmSWEET10* (drought: −3.57; waterlogging: −5.26) and *ZmSWEET19* (drought: −3.94; waterlogging: −3.84) showed reduced expression in roots of PML46 under both drought and waterlogging whereas, *ZmSWEET3* (drought: 0.87; waterlogging: 1.24) and *ZmSWEET7* (drought: 1.29; waterlogging: 7.20) showed higher expression. Likewise, CML563 showed upregulated expression of ZmSWEET*3, ZmSWEET7* and *ZmSWEET10* across the stresses and tissues, although the expression levels were quite low in a few cases. On the other hand, *ZmSWEET9* and *ZmSWEET19* showed both enhanced and down-regulated expression.

The degree of dominance was worked out for absolute expressions of *ZmSWEET3, ZmSWEET7, ZmSWEET9, ZmSWEET10* and *ZmSWEET19* in three hybrids (PML46 × CML563; LM13 × CML563 and PML69 × CML563) (Table 5). The degree of dominance of *ZmSWEET* genes was variable with genetic background, tissues and stress type, indicating the genotype-specific gene action in maize. Majorly the gene actions of *ZmSWEET* genes were non-additive in nature as the d/a ratio has deviated from zero (Table 5). However, *ZmSWEET10* in the waterlogged root and *ZmSWEET19* in the control roots and waterlogged shoots of PML46 × CML563 showed nearly additive gene action (d/a = 0.94 to 1.10). In support of variable dominance with tissues, the *ZmSWEET3* showed over-dominance under waterlogging stress in PML46 × CML563. Interestingly, complete overdominance was observed for the expression of *ZmSWEET7* across the treatments and tissues in PML46 × CML563. The *ZmSWEET19* expression showed partial to complete dominance
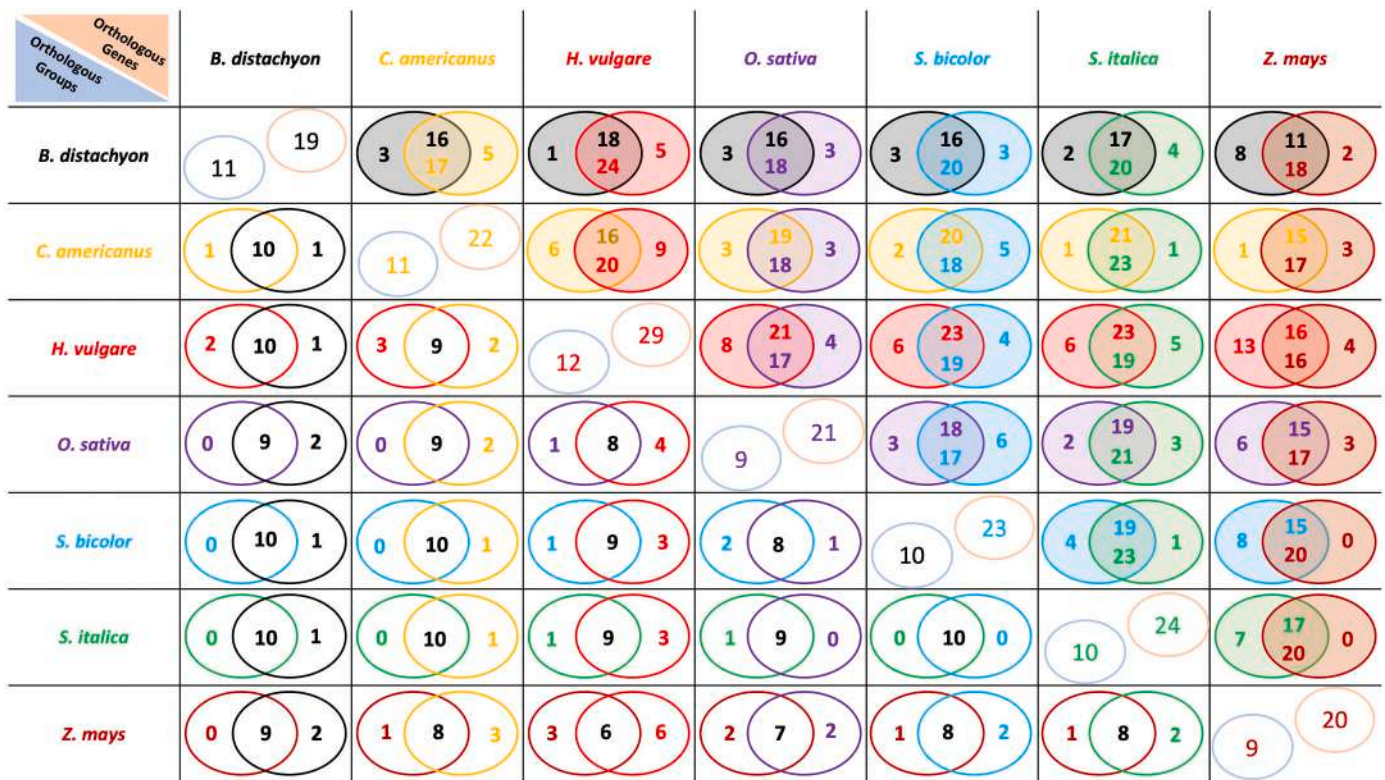
Fig. 5. The Venn diagrams depicting the pairwise comparison of SWEET repertories among the seven Poaceae members. The Venn diagrams in the bottom left shows number of orthogroups that are shared by the two species. The Venn diagrams in the upper right shows the homologous gene sequences that are common and specific to two species. The values in the lower and upper circles of diagonal squares indicate the total number of orthogroups and total number of SWEET genes in the respective species.

across the stresses and tissues. The mean d/a1 values were positive for the genes, *ZmSWEET7* (16.93), *ZmSWEET9* (18.64)*, ZmSWEET10* (57.4) and *ZmSWEET19* (4.01) and negative for *ZmSWEET3* (−2.49). Therefore, the results suggest that the maternal genotypes PML46, LM13 and PML69 contributed to expression values of *ZmSWEET7, ZmSWEET9, ZmSWEET10* and *ZmSWEET19* in hybrids whereas, CML563 contributed to the absolute expression of *ZmSWEET3*.

3.4.5. Co-expression analysis of SWEET genes in maize

The co-expression analysis showed 224 genes clustering with 19 co-expression *ZmSWEET* nodes in 10 co-expression clusters (A-J) (Fig. 10). The KEGG ontology of co-expressing genes with *ZmSWEETs* showed the involvement of several genes with benzoxazinoid biosynthesis (KEGG: zma00402; 5 genes), MAPK signaling pathway (KEGG: zma04016; 5 genes), plant hormone signal transduction (KEGG: zma04075; 5 genes), phenylpropanoid biosynthesis (KEGG: zma00940; 4 genes) and pentose and glucuronate inter-conversions (KEGG: zma00040; 4 genes).

The *salt tolerance-like protein* (LOC100273363) was found to be co-expressing with *ZmSWEET6* (*LOC100273190*), *ZmSWEET19* (*LOC100273779*) and *ZmSWEET20* (LOC100282708) in cluster B. Similarly, the genes *sodium transporter HKT1* (LOC100382359) in cluster C and *sodium/hydrogen exchanger 4* (LOC103638329) in cluster J were co-expressing neighbours with *ZmSWEET11* and *ZmSWEET7,* respectively. Further, *cold and drought-regulated protein CORA* (LOC109944797) showed co-expression with *ZmSWEET16* in cluster 2. Additionally, the important nutrient transporters viz., nitrogen transporters *protein nrt1/ptr family 1.1* (LOC103651182) and *protein nrt1/ptr family 4.3* (LOC103646286) were co-expressed with *ZmSWEET10* and *ZmSWEET2* in clusters A and C, respectively. Two phosphorous transporters, *phosphate transporter PHO1–2* (LOC103627883) and *phosphate transporter PHO1–3* (LOC103630022) of cluster B showed co-expression with *ZmSWEET4* and *ZmSWEET19*, respectively. Moreover, *ZmSWEETs*

co-expression analysis also showed various stress-associated transcription factor genes, viz. *MYB59* (LOC100283510), *Dof zinc finger protein DOF2.2* (*LOC100273654*), *MADS-box transcription factor 26* (*LOC103628959*), bHLH111 (*LOC103647665*) etc.

3.4.6. Regulatory network analysis of SWEET genes in maize

The *ZmSWEETs* regulatory network (GRN) was constructed with regulatory miRNAs and transcription factors (TF). Four regulatory pathways were used to realize the *SWEET* genes regulatory network in maize, viz. 1) miRNAs regulating *ZmSWEETs* (miRNA-gene); 2) TFs regulating *ZmSWEETs* (TF-Gene); 3) TFs regulating TFs of *ZmSWEETs* (TF-TF), and 4) miRNA regulating TFs of *ZmSWEETs* (Fig. 11). The topological attributes of *ZmSWEET* GRN revealed 301 nodes, 1512 edges with a 9.73 average number of neighbours, an average clustering coefficient of 0.119 and a characteristic path length of 2.904. The *ZmSWEETs* showed 140 and 146 edges with TFs and miRNAs, respectively. Whereas, 597 and 629 edges were found for TF-TF and miRNA-TF interactions. Among the edges with miRNA, zma-miR164 family members contributed maximum interactions (miRNA-gene: 25; miRNA-TF: 78). In the case of edges formed with TF, the AP2-EREBP family showed the highest interaction with *ZmSWEETs* (41) and TF of *ZmSWEETs* (178). Among the *ZmSWEET* genes, *ZmSWEET12* showed more edges (28) with TFs followed by *ZmSWEET3* (24). In contrast, no edges with TFs were identified for *ZmSWEET14* and *ZmSWEET17*. For miRNA-*ZmSWEET* interactions, *ZmSWEET7* showed maximum edges (25) followed by *ZmSWEET9* (16)*, ZmSWEET19* (15), *ZmSWEET4* (14) and *ZmSWEET17* (11) (Table S15).

Table 4
The mean and range of Ka/Ks ratio, divergence distance (DD) and divergence time (DT) among the among orthologs of Brachypodium, barley, foxtail millet, maize, pearl millet, rice and sorghum.

		BdSWEETs			CaSWEETs			HvSWEETs			OsSWEETs			SbSWEETs			SiSWEETs		
		Ka/Ks	DD	DT (MYA)	Ka/Ks	DD	DT (MYA)	Ka/Ks	DD	DT (MYA)	Ka/Ks	DD	DT (MYA)	Ka/Ks	DD	DT (MYA)	Ka/Ks	DD	DT (MYA)
CaSWEETs	Mean	0.38	0.23	33.21															
	Min.	0.17	0.13	18.03															
	Max.	0.64	0.34	50.74															
HvSWEETs	Mean	0.30	0.19	30.35	0.39	0.26	38.32												
	Min.	0.08	0.09	16.94	0.20	0.15	19.26												
	Max.	0.66	0.41	60.21	0.60	0.38	64.39												
OsSWEETs	Mean	0.33	0.23	36.84	0.34	0.26	40.60	0.36	0.28	43.16									
	Min.	0.12	0.10	17.16	0.14	0.13	17.03	0.10	0.13	19.12									
	Max.	0.69	0.43	69.33	0.57	0.41	65.56	0.68	0.47	81.42									
SbSWEETs	Mean	0.40	0.28	40.56	0.27	0.18	32.60	0.35	0.28	42.88	0.34	0.27	44.58						
	Min.	0.15	0.18	22.26	0.12	0.09	14.76	0.15	0.15	20.71	0.13	0.16	21.78						
	Max.	1.52	0.76	67.22	0.61	0.27	51.93	0.64	0.44	67.36	0.61	0.46	74.65						
SiSWEETs	Mean	0.35	0.23	35.01	0.27	0.08	14.23	0.38	0.25	38.71	0.33	0.25	39.92	0.27	0.17	29.40			
	Min.	0.13	0.13	18.10	0.05	0.03	6.03	0.14	0.15	17.30	0.15	0.12	17.92	0.10	0.09	12.34			
	Max.	0.52	0.34	53.72	0.50	0.31	52.81	0.67	0.40	63.03	0.54	0.44	64.51	0.53	0.32	49.71			
ZmSWEETs	Mean	0.33	0.25	39.23	0.32	0.21	34.09	0.34	0.28	43.56	0.38	0.27	39.90	0.27	0.11	20.51	0.31	0.19	31.27
	Min.	0.14	0.21	26.81	0.17	0.11	15.99	0.20	0.20	27.73	0.24	0.18	23.50	0.11	0.05	7.17	0.15	0.09	14.75
	Max.	0.54	0.29	52.34	0.64	0.34	67.16	0.52	0.47	85.96	0.59	0.47	73.84	0.63	0.18	42.23	0.63	0.35	73.31

Note: MYA, million years ago.

4. Discussion

4.1. SWEET genes in maize and Poaceae lineage

Sugars Will Eventually be Exported Transporters (SWEETs) are novel, widely distributed and are known to regulate the influx and the efflux of sugar into and out of cells. The present investigation mined 20, 23, 22, 24, 21, 29 and 19 *ZmSWEETs, SbSWEETs, CaSWEETs, SiSWEETs, HvSWEETs* and *BdSWEETs,* respectively, in the latest released genomes of respective species based on homology-based BLAST search and HMM search with PF03083 domain. The mined *SWEETs* numbers were in accordance with previous reports on rice [24], sorghum [55] and foxtail millet [23]. However, our systematic mining reported here 20 *ZmSWEET* genes in the latest release of the maize genome (v 5.0), which is slightly different from previously reported SWEET gene numbers in maize genome v.2 (23 *ZmSWEETs*) [13,56], v.3 (24 *ZmSWEETs*) [23] and v.4 (24 *ZmSWEETs*) [22]. These observed differences in the *ZmSWEET* numbers could be associated with improvements in fixing the patches, capturing missing gene space and scaffolds validation in the latest released genome versions. Our mining strategy also revealed 19 and 29 SWEET genes in *Brachypodium* and barley, respectively. Further, ZmSWEETs showed the 3–1-3 TM domain orientation and sub-cellular localization in the membrane of cells and various cellular structures, suggesting their potential role in transporting sugars across the membranes [57].

4.2. Modeling and molecular docking of ZmSWEETs showed key amino acid residues involved in ZmSWEET-sugar interactions

The molecular weights of ZmSWEETs varied from 22.66 to 43.26 kDa, which are *on par* with previous reports, viz. ~18.61 to ~59.71 kDa in crops of Fabaceae [58], 19.09 to 37.41 kDa in banana [59], 15.96 to 63.43 kDa in *Prunus* and 10.93 to 36.9 kDa in wheat [12,60]. The ZmSWEETs structures quality through Ramachandran plots showed that >96 % of residues were energetically most favoured. The pairwise superimposition among ZmSWEETs showed low root mean square deviation (RMSD) values (<2 Å), indicating quite similar and highly conserved structures. Probing the sugars binding pockets of maize SWEET proteins through molecular docking facilitated an understanding of the mechanisms and interactions involved in ZmSWEET-mediated sugar transport. The docking results revealed that 85 % of ZmSWEET-sugars interactions (68) exhibited at least one asparagine residue forming hydrogen bonds with sugar molecules (Table S11; Fig. S6-S9). The high affinity of asparagine to hydrogen bonds lies with the ability of the amide group to accept and donate two hydrogen bonds. Thus, asparagine is also reported as a common amino acid connecting carbohydrate molecules in glycoproteins [61,62]. Among the hydrophobic interactions, tryptophan residues were found in 85 % of ZmSWEET-sugars interactions (68), followed by phenylalanine and valine (Table S11; Fig. S6-S9). The side chains of tryptophan, phenylalanine and valine were composed mostly of carbon and hydrogen and found to repel the water molecules owing to tiny dipole moments [63]. The orthologs of ZmSWEET19 (AtSWEET11) and ZmSWEET6 (AtSWEET12) in Arabidopsis showed nine amino acid residues, viz. Ser22, Ser56, Trp60, Asn77, Asn197, Trp181, Ser177, Val146, and Ser143 involved in AtSWEET11/12-sucrose interactions [64]. Interestingly, our investigation also showed six amino acid residues viz., ser56, Trp60, Asn197, Trp181, Ser177, and Ser143 of ZmSWEET19 and ZmSWEET6 interacting with sucrose molecule (Table S11; Fig. S6-S9). Further, the proline residues at 24th and 44th positions in ZmSWEET13 showed interactions with fructose and sucrose sugars. The loss of conserved proline residues in AtSWEET1 (an ortholog of ZmSWEET13) affected the sugar transportation activity [65]. Thus, the interacting residues are functionally conserved and have important considerations while designing SWEETs mediated genetic enhancement programs in cereals.
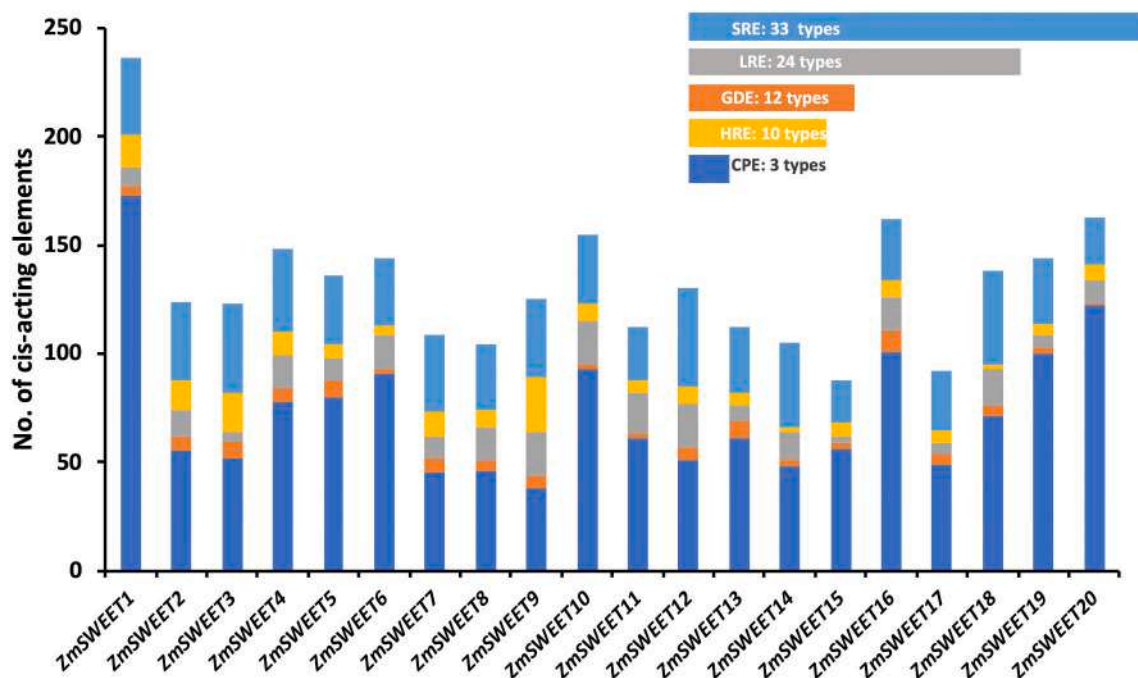
Fig. 6. The functional category and number of *cis*-acting elements predicted in the promoter sequences of *ZmSWEET* genes. The x-axis carries the *ZmSWEET* genes. The y-axis indicates the number of *cis*-acting elements identified in the promoter region, viz. core promoter elements (CPE), growth and development (GDE), light response (LRE), hormonal response (HRE) and stress response (SRE) elements. The length of legend bars are scaled to the diverse number *cis*-acting elements in that category. For detailed distribution of individual *cis*-acting elements among ZmSWEET promoter sequences please refer Table S14 and Figs. S15–19.

4.3. Evolution and divergence of the SWEET gene family in maize and cereal lineage

4.3.1. Segmental duplication contributed to the expansion and functional diversifications of ZmSWEETs under purifying selection

The gene family expansions in the evolution provide the raw material for coping-up with the fluctuating environment [66]. We have identified 13 pairs of segmental duplications and one pair of tandem duplications (*ZmSWEET19-ZmSWEET20*). The current results were in alignment with the regular trend of a greater number of segmentally duplicated genes over tandem duplications in plants [67] and contributed to the expansion of *NBS* [68], *HD-Zip* [69] and *PHD-Finger* [70] families in maize. Further, a moderate negative association of tandem and segmental duplications was reported in the fifty gene families of Arabidopsis [71].

The functional diversification of duplicated genes in the evolutionary trajectories occurs through non-functionalization (loss of function), neofunctionalization (acquiring new function) owing to coding and regulatory sequence, sub-functionalization (gene function partitioning), specialization (maintaining a new function along with ancestral functions) and maintaining the intact and structural copies without change [72]. The current study indicated the functional diversification of SWEET duplications and subsequent divergence under strong purifying selection. The duplication pairs *ZmSWEET2-ZmSWEET18* evolved under purifying selection, where the higher expression of *ZmSWEET2* was found in the embryo, germinating kernels and moderate expression in the root elongation zone; however, the expression of *ZmSWEET18* not observed in any of the tissues of B73, although minimal expression was observed in kernels of diverse maize inbred lines, indicating probable non-functionalization of *ZmSWEET18* in B73 lineage owing one TM1 domain loss. Neo-functionalization of *ZmSWEET5-ZmSWEET14* duplication pairs were owing to differential expression of *ZmSWEET5* and *ZmSWEET14* in leaf and root tissues, respectively. A similar kind of functional diversification was observed between *ZmSWEET8* (mature pollen and silk tissues) and *ZmSWEET17* (internodes). Interestingly, the expression pattern of *ZmSWEET19-ZmSWEET20* and *ZmSWEET10-*

ZmSWEET12 in common and different tissues of maize organs indicated the specialization of duplicated pairs. In Arabidopsis, duplicated genes mostly showed novel developmental regulatory patterns [73] and environmental responses [74]. Similarly, the duplicated genes in maize showed novel leaf gene expression patterns via regulatory neo-functionalization [75].

4.3.2. Conservation of SWEETs in the evolutionary lineage of cereals

An evolutionary understanding of the *SWEET* family in cereal lineage revealed the limited expansion and conserved nature of *SWEET* genes in cereals. The whole genome collinearity was observed in accordance with current cereals genome evolutionary patterns, i.e., maximum collinearity between the pairs of maize-sorghum, followed by foxtail millet-sorghum, maize-foxtail millet and *Brachypodium*-foxtail millet. However, maximum *SWEET*-collinear blocks between foxtail millet-sorghum followed by maize-foxtail millet and maize-sorghum indicated the loss of collinear blocks or orthologous *SWEET* genes during maize and sorghum divergence or domestication process. In support of this, Lai [76] reported that at least 50 % of the duplicated genes from the maize progenitors were lost within 5 million years.

Being identical by descent, orthologs might have conserved their function or may functionally diverge into different species gene duplication events under selection pressure [77,78]. The pairwise comparison of OGs and orthologous sequence showed a highly conserved nature of *SWEET* genes in the cereals' lineage. For instance, rice, sorghum and foxtail millet shared all the OGs with *Brachypodium* and pearl millet. Similarly, 100 % OG sharing was found between sorghum and foxtail millet; however, the lowest OG share was found in barley-maize (50 %) and barley-rice (66 %) as against 75–100 % OG sharing among all other combinations. In support, except *CaSWEETs* with *ZmSWEETs* and *HvSWEETs*, 80–100 % of *SWEETs* of target species were orthologs, suggesting conserved orthology of *SWEETs* in the cereals' lineage. Interestingly, the results of the phylogenetic analysis were in accordance with the orthology-based grouping pattern. For instance, OG00 sub-clusters were exactly in accordance with sub-clusters (Ia, Ib, Id) of cluster-I and cluster-II. Each ortholog group contain genes from different
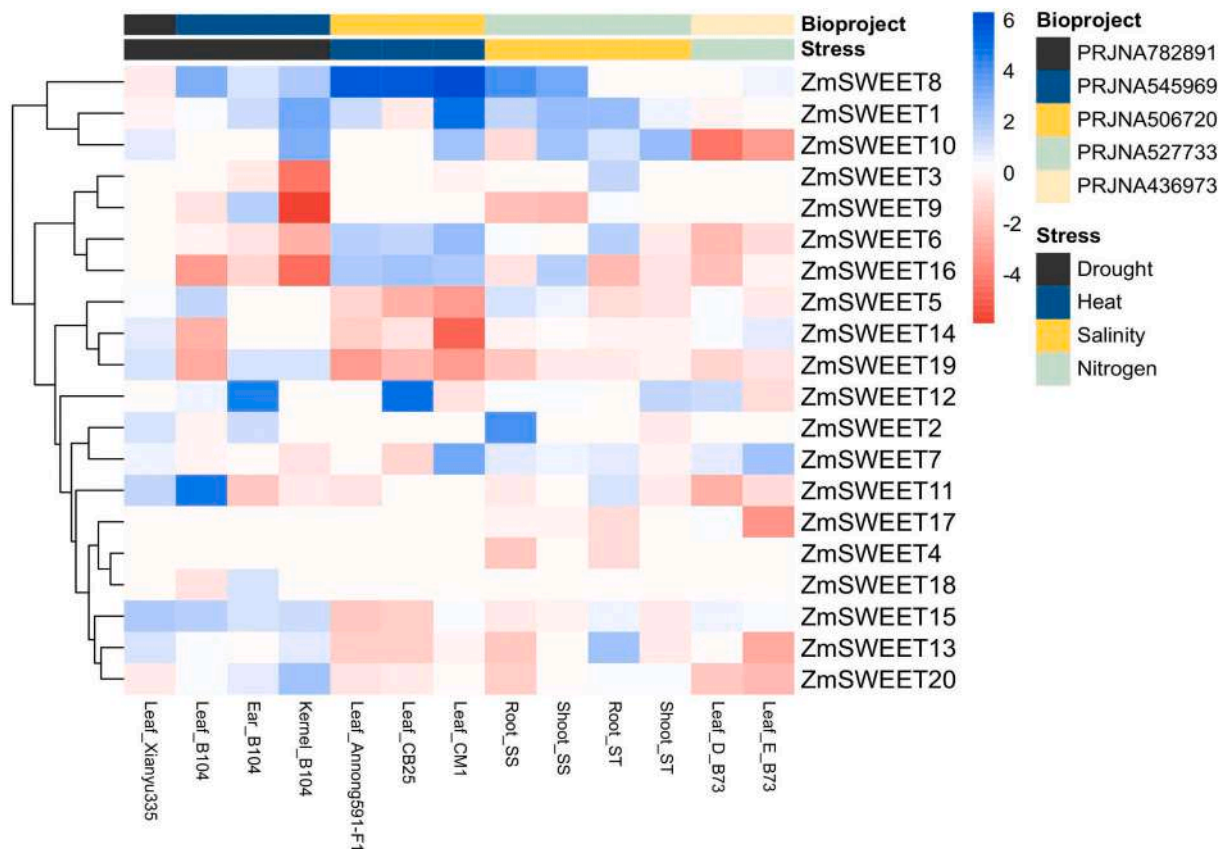
Fig. 7. *Spatial in-silico* expression of SWEET genes in maize: (A) The heat map showing the expression of *ZmSWEET* genes in various tissues of classical maize inbred line B73, (B-E) The heat maps showing the expression of *ZmSWEET* genes in kernel of maize inbred lines belonging to four sub-populations: (B) TST, (C) NSS, (D) Mixed and (E) SS. All the expression datapoints are presented as FPKM values.

species and provides valuable information on biological function [79]. The genes in OGs are highly clustered with minimal duplication and deletion events and are termed persistent genes [80] and are mostly evolved under strong selective pressure with high functional consistency [79]. Strong purifying selection is ubiquitous in natural populations and

is mainly responsible for conserving genomic sequences and preserving biological functions across long evolutionary timescales [81]. The *SWEETs* are very important to carry out the basic sugar and carbohydrate metabolism in plants. Any disruptions in *SWEET* genes may affect the plant system. For instance, the knock-out of *ZmSWEET13a, b,* and *c*

Fig. 8. *In-silico* expression of *SWEET* genes in response to various abiotic stresses in maize: Heat maps showing expression of *SWEET* genes in maize during drought, heat, salinity, and nitrogen stresses. The data shows *log2fold* values of expression. The fold change values of each gene expressions were computed through comparing with to plants grown under control or optimum environment.

Fig. 9. *In-silico* expression of *SWEET* genes in response to various abiotic stresses in maize: Heat maps showing expression of *SWEET* genes in maize during drought, heat, salinity, and nitrogen stresses. The data shows *log2fold* values of expression. The fold change values of each gene expressions were computed through comparing with to plants grown under control or optimum environment.

resulted in severely stunted phenotype, impaired phloem loading, reduced photosynthetic activity, and disturbed soluble sugars and starch distribution [82]. Similarly, the mutants of *SWEET4* [13], *SWEET11* and *SWEET15* [83] severely impaired the grain filling in rice.

4.4. Expression and co-expression analyses showed the role of ZmSWEETs in growth and abiotic stress regulation in maize

4.4.1. Plant growth and kernel formation

The *SWEET*s were showed to play an important physiological and developmental processes, including long-distance sugar transport, pollen nutrition and seed filling. The enhanced expression of paralogs *ZmSWEET6*, *ZmSWEET19* and *ZmSWEET20* in mature leaf is associated with sucrose loading to phloem and the knockout events of these

Table 5
The dominance by additivity ratios (d/a1; −d/a2) of *ZmSWEET* genes in target heterotic combinations under drought and waterlogging stresses.

Hybrid	Stress-Tissue	ZmSWEET19		ZmSWEET10		ZmSWEET7		ZmSWEET3		ZmSWEET9	
		d/a1	d/a2	d/a1	d/a2	d/a1	d/a2	d/a1	d/a2	d/a1	d/a2
PML46 × CML563	C-S	0.58	−0.58	5.12	−5.12	−7.99	7.99	1.50	−1.50	−8.81	8.81
PML46 × CML563	C-R	1.10	−1.10	3.42	−3.42	17.06	−17.06	7.10	−7.10	2.45	−2.45
PML46 × CML563	D-S	−0.19	0.19	−6.47	6.47	−31.12	31.12	0.83	−0.83	−1.60	1.60
PML46 × CML563	D-R	0.81	−0.81	12.49	−12.49	14.61	−14.61	−1.24	1.24	−8.77	8.77
PML46 × CML563	W-S	1.11	−1.11	0.69	−0.69	14.77	−14.77	−5.95	5.95	11.87	−11.87
PML46 × CML563	W-R	1.22	−1.22	0.94	−0.94	11.28	−11.28	−1.19	1.19	−0.44	0.44
LM13 × CML563	C-S	−0.04	0.04	0.68	−0.68	−15.41	15.41	1.16	−1.16	4.24	−4.24
LM13 × CML563	C-R	0.46	−0.46	0.92	−0.92	1.61	−1.61	2.28	−2.28	0.86	−0.86
LM13 × CML563	D-S	0.90	−0.90	−3.60	3.60	1.95	−1.95	−0.13	0.13	−10.68	10.68
LM13 × CML563	D-R	0.96	−0.96	17.96	−17.96	1.74	−1.74	0.63	−0.63	21.58	−21.58
LM13 × CML563	W-S	1.06	−1.06	0.23	−0.23	2.09	−2.09	−4.74	4.74	47.36	−47.36
LM13 × CML563	W-R	1.01	−1.01	−2.69	2.69	2.20	−2.20	0.53	−0.53	0.57	−0.57
PML69 × CML563	C-S	−0.99	0.99	23.69	−23.69	−0.02	0.02	2.19	−2.19	7.23	−7.23
PML69 × CML563	C-R	−0.89	0.89	−0.92	0.92	−1.17	1.17	−0.65	0.65	−1.19	1.19
PML69 × CML563	D-S	−0.49	0.49	0.68	−0.68	−0.28	0.28	−1.87	1.87	−41.44	41.44
PML69 × CML563	D-R	−0.82	0.82	−0.88	0.88	−1.18	1.18	−1.52	1.52	−1.26	1.26
PML69 × CML563	W-S	−0.59	0.59	5.23	−5.23	1.64	−1.64	0.07	−0.07	−0.97	0.97
PML69 × CML563	W-R	−1.19	1.19	−0.09	0.09	5.15	−5.15	−1.49	1.49	−2.36	2.36

Note: C, control; D, drought; W, waterlogging; S, shoot; R, root.

paralogous severely affected the plant architecture and enhanced sucrose accumulation in leaves [82]. The *SWEETs* were also involved in seed filling, helping to transfer nutrients to the growing embryo. The ZmSWEET4c and OsSWEET4, the paralogs of ZmSWEET11 and ZmSWEET12, showed enhanced expression in embryo, endosperm and kernels which clearly established that these SWEETS mediate the kernel filling in maize [13]. The sugar and starch metabolisms are crucial in regulating pollen nourishment, germination and pollen tube growth. The mature pollens of B73 showed higher expression of *ZmSWEET8*. Similarly, the higher expression of *Xa13* was reported in panicles and anthers showed reduced fertility in mutant lines for *Xa13* [84].

4.4.2. Drought and salinity stress

The higher expression of *SWEETs* is associated with increased sugar mobilization and accumulation [85]. The sugars accumulation under drought and salinity stresses enhances the plant's adaptability through stomatal closure, turgidity and water level maintenance in leaves and reduces the oxidative damage to cell membranes [86,87]. The *AtSWEET11* and *AtSWEET12,* the orthologs (many-to-many) of *ZmSWEET3, ZmSWEET9, ZmSWEET10*, and *ZmSWEET19* showed to alter the shoot-to-root ratios under drought [87]. Further, the higher expression of *OsSWEET13,* which is an ortholog of *ZmSWEET6, ZmSWEET19,* and *ZmSWEET20,* showed enhanced expression under drought stress in root and shoot tissues [88].

The co-expression of drought-responsive genes, viz. *cold and drought-regulated protein* (*LOC109944797*) with *ZmSWEET16* in cluster B, *dehydrin COR410* (*LOC100281087*) with *ZmSWEET1* in cluster F, *tonoplast intrinsic protein 3* (TIP3; *LOC541912*) with *ZmSWEET11* in cluster C etc. were observed in the co-expression network. Similarly, key salinity stress-associated genes *HKT1* (*LOC100382359*) and *salt tolerance-like protein* (*LOC100273363*) were co-expressed in cluster B and cluster J, respectively (Fig. 10). The overexpression of the *cold and drought regulatory-protein encoding CORA-like* (CRD) from *Salicornia brachiate* in tobacco resulted in tolerance against salinity, drought and cold stresses through enhanced chlorophyll contents, plant biomass and sugars accumulation [89]. Similarly, the higher expression of *CORA-like* genes was reported under drought and elevated Co_2 stresses in sweet potato [90] and in *Citrus limonia* under salinity stress [91]. In wheat, *COR410* showed to protect the plasma membrane against freezing and dehydration stress [92]. HKT1 sodium transporters mediate high-affinity Na^+–K^+ co-transport and preferred Na^+-selective low-affinity Na^+ transport in plants [93]. Under salinity stresses, the Arabidopsis and rice *AtHKT–1* and *OsHKT1–5* mediate the Na^+ exclusion from leaves [94,95].

4.4.3. Waterlogging stress

Waterlogging stress showed enhanced expression of *ZmSWEET3, ZmSWEET7, ZmSWEET9* and *ZmSWEET10* in root and shoot of CML563, PML93 and LM13 × CML563. The waterlogging resulted in contrasting expression of *ZmSWEETs* in root tissues of PML93 and sensitive PML10 (Fig. 9). The waterlogging tolerant rice and pigeon pea lines showed enhanced accumulation of sugars [96,97], which subsequently induced the formation of adventitious root through promoting auxin transport and signaling events [98]. Interestingly, the co-expression network also showed the expression of *auxin response factor 1* (*LOC100857063*) with *ZmSWEET9* in cluster A. Further, except roots of sensitive genotypes PML10 and PML69, all the genotypes showed enhanced expression of *ZmSWEET9* under waterlogging stress (Fig. 9) and intense expression in primary and secondary roots of B73 (Fig. 7A). The binding of MaRAP2–4 to *DRE* and/or *GCC box* of *AtSWEET10*, a *ZmSWEET9* ortholog, regulated sugar availability and waterlogging tolerance [99]. Additionally, the presence of *DRE element* in the promoter region supported the possible role of *ZmSWEET9* in waterlogging tolerance.

4.4.4. Heat stress

The heat stress in plants enhances the accumulation of non-structural carbohydrates and total sugars [100]. During the reproductive phase, heat stress affects starch synthesis enzyme activities and results in an increased accumulation of sugars meant for starch synthesis [101]. Additionally, the heat stress reduced starch content in tomato mesophyll cells [102]. Thus, heat stress resulted in enhanced expression of *ZmSWEET6, ZmSWEET8* and *ZmSWEET16* in the leaves (Fig. 8). The pollens are very sensitive to heat stress in maize and prominent expression of *ZmSWEET8* in the pollen tissues of B73, indicating its candidature in breeding heat-tolerant cultivars.

4.4.5. Nutritional stress

Phosphorus and potassium deficiencies were found to result in sucrose accumulation in leaves and decreased phloem-mediated sugars transportation and subsequent growth impairment [103]. Nitrogen starvation resulted in downregulated expression of most of the *ZmSWEET* genes except for *ZmSWEET7* and *ZmSWEET12* in the leaf tissues of B73 (Fig. 8). Nitrogen starvation severely affects the chlorophyll concentration, which in turn affects photosynthesis and subsequently sugar synthesis and their phloem-mediated transport in the plant system. Thus, the activity of *ZmSWEETs* could have been repressed
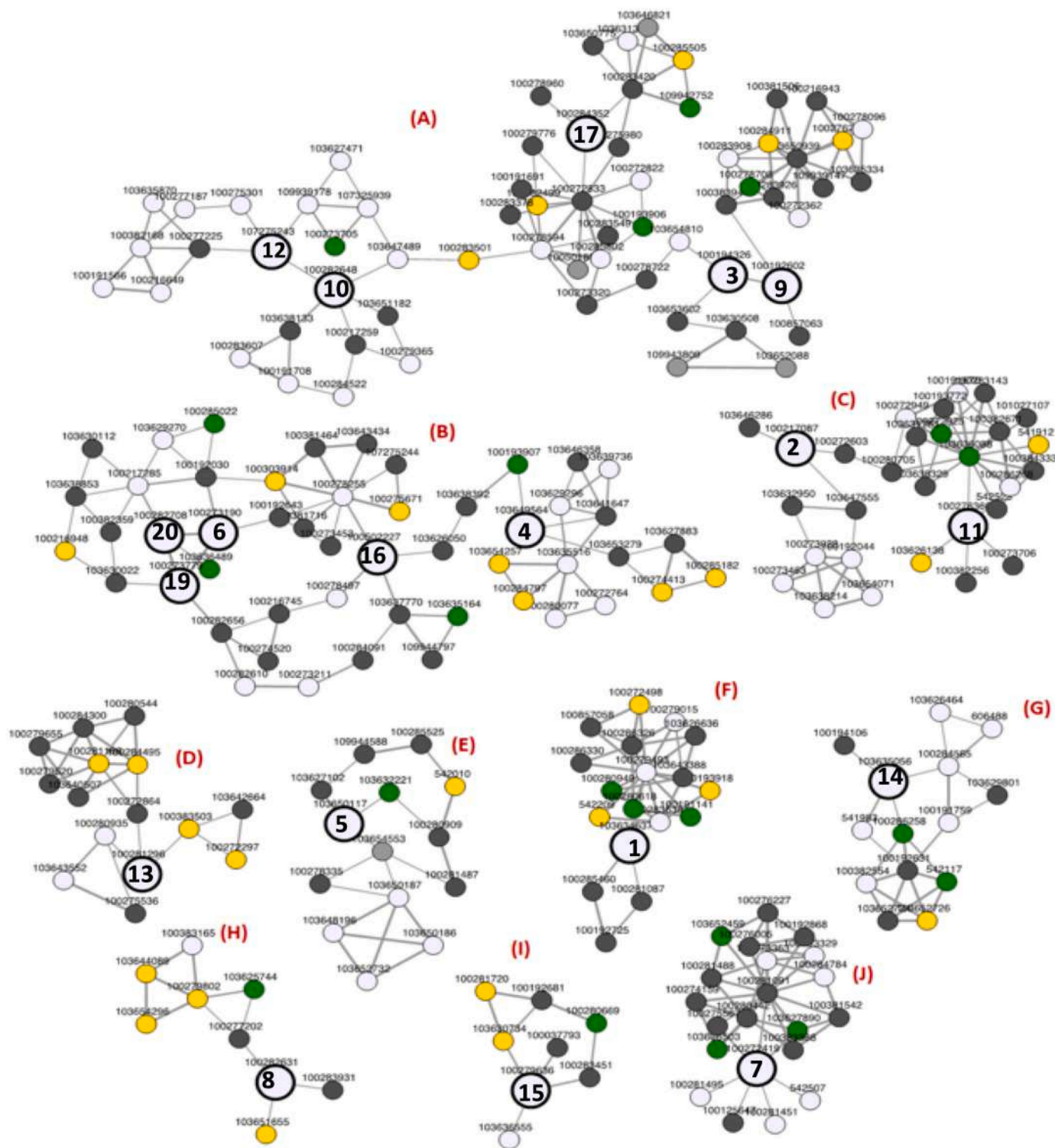
Fig. 10. The co-expression network of *ZmSWEET* genes. The co-expression network showed 224 genes clustered with 19 *ZmSWEET* nodes in the ten co-expression clusters. The bold number in circle indicates the respective ZmSWEETs.

during nitrogen starvation. In co-expression analysis, genes belonging to nitrogen transporters, viz. *NRT1/PTR1.1* (*LOC103651182*) in cluster A and *NRT1/PTR4.3* (*LOC103646286*) in cluster C were expressing with *ZmSWEET10* and *ZmSWEET2*, respectively. Further, the cluster B showed phosphorous (*PHO1–3, LOC103630022; PHO1–2, LOC103627883*) and potassium transporter (*probable potassium transporter 4, LOC103653279*) genes co-expressing with *ZmSWEET6, ZmSWEET19, ZmSWEET20* and *ZmSWEET4* (Fig. 10), indicating the

strong linkage between sugar and mineral metabolism.

4.5. The dominance of ZmSWEETs expression is governed by genetic backgrounds, kind of tissues and stress-type

The expression of superior allele(s) associated with target traits is the genetic basis for dominant trait expression in hybrids for the exploitation of heterosis [104]. Additionally, the heterosis-associated gene
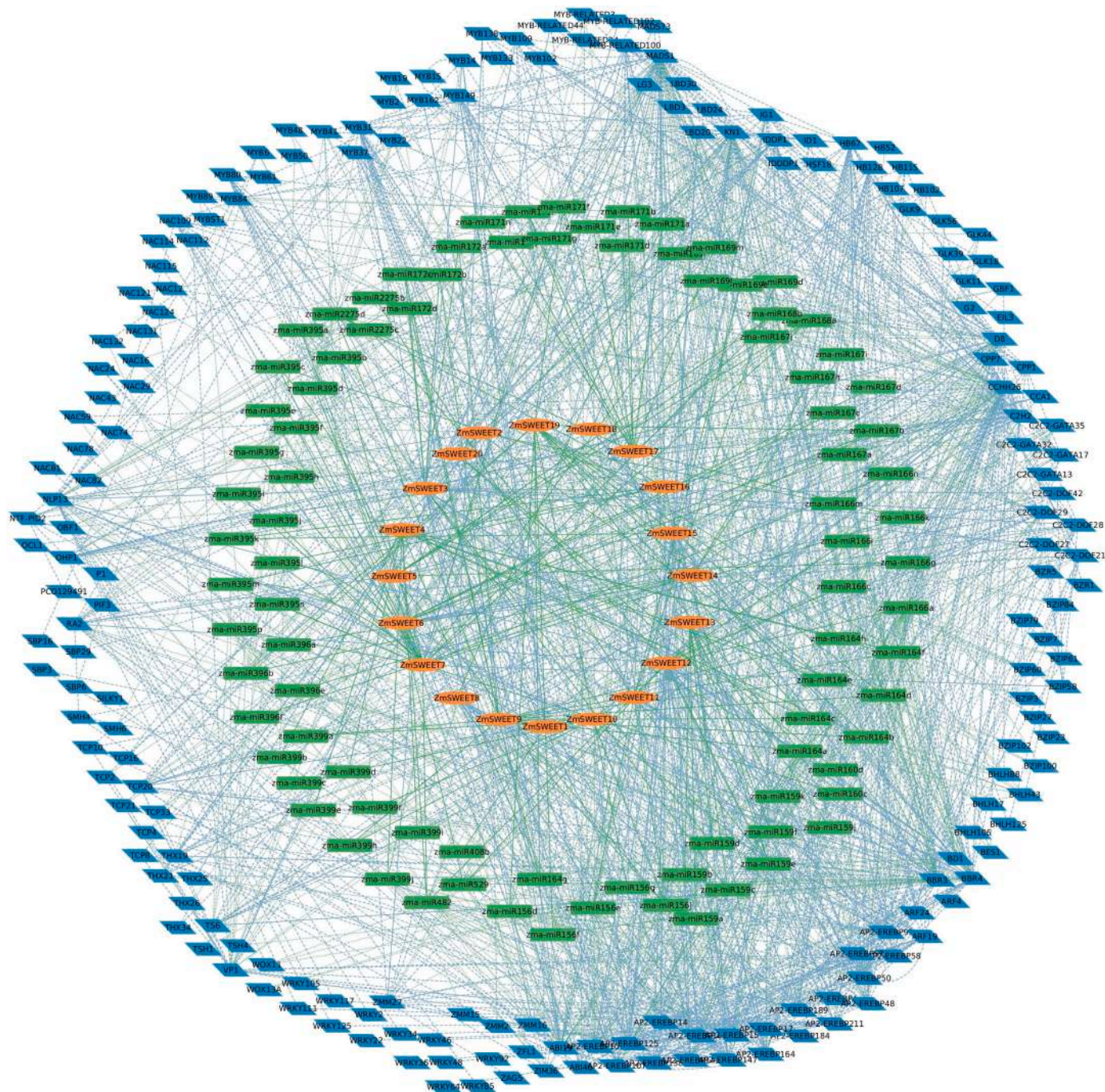
Fig. 11. The genes regulatory network showing various interactions snapshots involved in regulations of *ZmSWEETs* expression. The TFs, miRNAs and ZmSWEETs are represented with parallelogram, rectangle and ellipses, respectively. The *ZmSWEET*-TF, *ZmSWEET*-miRNA, TF-miRNA and TF-TF (TF of TF regulating *ZmSWEETs*) are represented with blue-continuous, green-continuous, green-dotted and Blue-dotted, respectively.

expression patterns are influenced by various factors, viz. gene-regulatory interactions among parental alleles [105], complex transcriptional networks specific to developmental stages and tissues [106], multiple biological processes, DNA sequence variation [107], gene copy numbers [108] etc.

The *ZmSWEETs* mostly showed over-dominance gene actions, although few cases showed additivity against dominance, viz. *ZmSWEET3* (waterlogged shoot) and *ZmSWEET10* (waterlogged root) in PML69 × CML563 and *ZmSWEET19* in the shoots of control. The quantitative nature of non-additive gene expression is the major driving force for heterosis under stress conditions, although hybrids do possess additive complementation as an intrinsic property [49,109]. The degree

of dominance of five *ZmSWEET* genes was variable with the genetic background of parental lines and hybrid, the kind of tissues and stress. For instance, within PML46 × CML563 hybrid, *ZmSWEET7* showed over-dominance gene action across treatments and tissues whereas, *ZmSWEET3, ZmSWEET9, ZmSWEET10* and *ZmSWEET19* showed partial, complete and over-dominant gene actions (Table 5). Current investigation revealed the range of non-additive gene action of SWEET genes, which implies that different kinds of regulatory and molecular mechanisms mediate this variation. Studies in *Drosophila* [110], *Arabidopsis* [111] and maize [112] showed the expression of genes beyond the parental range, indicating the presence of novel gene regulation in the hybrids [112]. Further, the variation in regulatory elements

composition among the different genotypes could also add to expression variation and subsequent gene actions [113]. The *ZmSWEET3* showed tissue-associated gene action variation in shoot and root of control and waterlogged stress in the hybrids LM13 × CML563 and PML69 × CML563. The same was observed for *ZmSWEET7* under waterlogging stress in PML69 × CML563 (Table 5). The tissue-specific expression pattern of genes is one of the factors influencing the nature of gene action and differential regulation of tissue development to modulate stress tolerance [114,115]. Further, the change in the gene actions among the stresses could be associated with the complex regulatory patterns associated with intricate drought and waterlogging tolerance component traits, which are mostly interlinked [116]. The gene action of *SWEET* genes under stress conditions could also be determined by a range of post-transcriptional events, viz. splicing, translation, protein folding and stabilisation [50]. Additionally, the role of small RNAs such as micro-RNA (miRNAs) and small interfering RNA (siRNA) cannot be ignored [116]. For instance, *ZmSWEETs* associated miRNAs, viz. zma-miR164e (*ZmSWEET9* and *ZmSWEET19*) [117] and zma-miR168a, b (*ZmSWEET7*) [118] showed waterlogging and drought regulation.

5. Conclusion

We report here a total of 20 *ZmSWEET* genes in the latest maize genome release (*v.5*). The molecular docking of ZmSWEETs clearly established that asparagine, valine, tryptophan, serine and proline as key amino acids involved in ZmSWEET-sugar interactions and are of potential interest to undertake CRISPR/*Cas* mediated editing and transgenic studies to modulate the sugar transport system in maize. The *SWEET* gene family in cereals has been proved to be conserved and shaped under purifying selection with various functionalization events. The expression and co-expression analyses showed the regulatory role of *ZmSWEETs* in assigning tolerance to abiotic stresses. Further, the presence of diverse *cis*-acting elements, regulatory elements and gene action studies showed the role of genetic background, regulatory elements, kind of stresses and tissues on functional diversification and dominance behaviour of *ZmSWEET* transporters. Our findings have paved the strong base for subsequent in-depth studies on *ZmSWEETs* in growth and stress tolerance using various functional validation approaches and genetic improvement of maize and other cereals.

CRediT authorship contribution statement

P.N. Vinodh Kumar: Data curation, Investigation, Formal Analysis, Writing- Original draft preparation. Mallana Gowdra Mallikarjuna: Conceptualization, Methodology, Funding acquisition, Supervision, Writing- Original draft preparation, Writing – review & editing. Shailendra Kumar Jha: Data curation, Writing – review & editing. Anima Mahato: Data curation, Writing – review & editing. Shambhu Krishan Lal: Data curation, Writing – review & editing. Yatish K.R.: Investigation; Hirenallur Chandappa Lohithaswa: Data curation, Writing – review & editing. Viswanathan Chinnusamy: Funding acquisition, Supervision, Writing – review & editing.

Declaration of competing interest

The authors declare that they have no known competing financial interests or personal relationships that could have appeared to influence the work reported in this paper.

Data availability

All the raw data sets were downloaded from publicly available databases. The rest of the supporting data sets are provided as supplementary files.

Appendix A. Supplementary data

Supplementary data to this article can be found online at https://doi.org/10.1016/j.ijbiomac.2022.12.326.

References

[1] F. Rolland, E. Baena-Gonzalez, J. Sheen, Sugar sensing and signaling in plants: conserved and novel mechanisms, Annu. Rev. Plant Biol. 57 (2006) 675–709, https://doi.org/10.1146/ANNUREV.ARPLANT.57.032905.105441.

[2] L.Q. Chen, L.S. Cheung, L. Feng, W. Tanner, W.B. Frommer, in: Transport of Sugars 84, 2015, pp. 865–894, https://doi.org/10.1146/ANNUREV-BIOCHEM-060614-033904.

[3] S. Gazzarrini, P. McCourt, Genetic interactions between ABA, ethylene and sugar signaling pathways, Curr. Opin. Plant Biol. 4 (2001) 387–391, https://doi.org/10.1016/S1369-5266(00)00190-4.

[4] M. Wang, L. Zang, F. Jiao, M.D. Perez-Garcia, L. Ogé, L. Hamama, J. le Gourrierec, S. Sakr, J. Chen, Sugar signaling and post-transcriptional regulation in plants: an overlooked or an emerging topic? Front. Plant Sci. 11 (2020) 1636, https://doi.org/10.3389/FPLS.2020.578096.

[5] Y.-L. Ruan, Sucrose metabolism: gateway to diverse carbon use and sugar signaling, Annu. Rev. Plant Biol. 65 (2014) 33–67, https://doi.org/10.1146/annurev-arplant-050213-040251.

[6] Y. Wei, D. Xiao, C. Zhang, X. Hou, The expanded SWEET gene family following whole genome triplication in Brassica rapa, Genes (Basel) 10 (2019), https://doi.org/10.3390/GENES10090722.

[7] R. Lemoine, S. la Camera, R. Atanassova, F. Dédaldéchamp, T. Allario, N. Pourtau, J.L. Bonnemain, M. Laloi, P. Coutos-Thévenot, L. Maurousset, M. Faucher, C. Girousse, P. Lemonnier, J. Parrilla, M. Durand, Source-to-sink transport of sugar and regulation by environmental factors, Front. Plant Sci. 4 (2013) 272, https://doi.org/10.3389/FPLS.2013.00272.

[8] Y.H. Xuan, Y.B. Hu, L.Q. Chen, D. Sosso, D.C. Ducat, B.H. Hou, W.B. Frommer, Functional role of oligomerization for bacterial and plant SWEET sugar transporter family, Proc. Natl. Acad. Sci. U. S. A. 110 (2013) E3685–E3694, https://doi.org/10.1073/PNAS.1311244110.

[9] L. Feng, W.B. Frommer, Structure and function of SemiSWEET and SWEET sugar transporters, Trends Biochem. Sci. 40 (2015) 480–486, https://doi.org/10.1016/J.TIBS.2015.05.005.

[10] L.Q. Chen, B.H. Hou, S. Lalonde, H. Takanaga, M.L. Hartung, X.Q. Qu, W.J. Guo, J.G. Kim, W. Underwood, B. Chaudhuri, D. Chermak, G. Antony, F.F. White, S. C. Somerville, M.B. Mudgett, W.B. Frommer, Sugar transporters for intercellular exchange and nutrition of pathogens, Nature 468 (2010) 527–532, https://doi.org/10.1038/nature09606, 2010 468:7323.

[11] G. Patil, B. Valliyodan, R. Deshmukh, S. Prince, B. Nicander, M. Zhao, H. Sonah, L. Song, L. Lin, J. Chaudhary, Y. Liu, T. Joshi, D. Xu, H.T. Nguyen, Soybean (Glycine max) SWEET gene family: insights through comparative genomics, transcriptome profiling and whole genome re-sequence analysis, BMC Genomics 16 (2015) 1–16, https://doi.org/10.1186/S12864-015-1730-Y.

[12] Y. Gao, Z.Y. Wang, V. Kumar, X.F. Xu, D.P. Yuan, X.F. Zhu, T.Y. Li, B. Jia, Y. H. Xuan, Genome-wide identification of the SWEET gene family in wheat, Gene 642 (2018) 284–292, https://doi.org/10.1016/J.GENE.2017.11.044.

[13] D. Sosso, D. Luo, Q.B. Li, J. Sasse, J. Yang, G. Gendrot, M. Suzuki, K.E. Koch, D. R. McCarty, P.S. Chourey, P.M. Rogowsky, J. Ross-Ibarra, B. Yang, W.B. Frommer, Seed filling in domesticated maize and rice depends on SWEET-mediated hexose transport, Nat. Genet. 47 (2015) 1489–1493, https://doi.org/10.1038/ng.3422, 2015 47:12.

[14] H.Y. Chen, J.H. Huh, Y.C. Yu, L.H. Ho, L.Q. Chen, D. Tholl, W.B. Frommer, W. J. Guo, The Arabidopsis vacuolar sugar transporter SWEET2 limits carbon sequestration from roots and restricts Pythium infection, Plant J. 83 (2015) 1046–1058, https://doi.org/10.1111/TPJ.12948.

[15] G. Antony, J. Zhou, S. Huang, T. Li, B. Liu, F. White, B. Yang, Rice xa13 recessive resistance to bacterial blight is defeated by induction of the disease susceptibility gene Os-11N3, Plant Cell 22 (2010) 3864–3876, https://doi.org/10.1105/TPC.110.078964.

[16] M. Hutin, A.L. Pérez-Quintero, C. Lopez, B. Szurek, MorTAL Kombat: the story of defense against TAL effectors through loss-of-susceptibility, Front. Plant Sci. 6 (2015) 535, https://doi.org/10.3389/FPLS.2015.00535.

[17] J. Zhou, Z. Peng, J. Long, D. Sosso, B. Liu, J.S. Eom, S. Huang, S. Liu, C. Vera Cruz, W.B. Frommer, F.F. White, B. Yang, Gene targeting by the TAL effector PthXo2 reveals cryptic resistance gene for bacterial blight of rice, Plant J. 82 (2015) 632–643, https://doi.org/10.1111/TPJ.12838.

[18] K.L. Cox, F. Meng, K.E. Wilkins, F. Li, P. Wang, N.J. Booher, S.C.D. Carpenter, L. Q. Chen, H. Zheng, X. Gao, Y. Zheng, Z. Fei, J.Z. Yu, T. Isakeit, T. Wheeler, W. B. Frommer, P. He, A.J. Bogdanove, L. Shan, TAL effector driven induction of a SWEET gene confers susceptibility to bacterial blight of cotton, Nat. Commun. 8 (2017) 1–14, https://doi.org/10.1038/ncomms15588, 2017 8:1.

[19] P.J. Seo, J.M. Park, S.K. Kang, S.G. Kim, C.M. Park, An Arabidopsis senescence-associated protein SAG29 regulates cell viability under high salinity, Planta 233 (2011) 189–200, https://doi.org/10.1007/S00425-010-1293-8.

[20] R. le Hir, L. Spinner, P.A.W. Klemens, D. Chakraborti, F. de Marco, F. Vilaine, N. Wolff, R. Lemoine, B. Porcheron, C. Géry, E. Téoulé, S. Chabout, G. Mouille, H. E. Neuhaus, S. Dinant, C. Bellini, Disruption of the sugar transporters AtSWEET11 and AtSWEET12 affects vascular development and freezing tolerance in Arabidopsis, Mol. Plant 8 (2015) 1687–1690, https://doi.org/10.1016/J. MOLP.2015.08.007.

[21] J. Ji, L. Yang, Z. Fang, Y. Zhang, M. Zhuang, H. Lv, Y. Wang, Plant SWEET family of sugar transporters: structure, evolution and biological functions, Biomolecules 12 (2022), https://doi.org/10.3390/BIOM12020205.

[22] M. López-Coria, T. Sánchez-Sánchez, V.H. Martinez-Marcelo, G.P. Aguilera-Alvarado, M. Flores-Barrera, B. King-Díaz, S. Sanchez-Nieto, SWEET transporters for the nourishment of embryonic tissues during maize germination, Genes (Basel) 10 (2019), https://doi.org/10.3390/GENES10100780.

[23] Z. Liu, H. Fan, Z. Ma, Comparison of SWEET gene family between maize and foxtail millet through genomic, transcriptomic, and proteomic analyses, Plant Genome 15 (2022), e20226, https://doi.org/10.1002/TPG2.20226.

[24] M. Yuan, S. Wang, Rice MtN3/saliva/SWEET family genes and their homologs in cellular organisms, Mol. Plant 6 (2013) 665–674, https://doi.org/10.1093/MP/ SST035.

[25] K.L. Howe, B. Contreras-Moreira, N. de Silva, G. Maslen, W. Akanni, J. Allen, J. Alvarez-Jarreta, M. Barba, D.M. Bolser, L. Cambell, M. Carbajo, M. Chakiachvili, M. Christensen, C. Cummins, A. Cuzick, P. Davis, S. Fexova, A. Gall, N. George, L. Gil, P. Gupta, K.E. Hammond-Kosack, E. Haskell, S.E. Hunt, P. Jaiswal, S.H. Janacek, P.J. Kersey, N. Langridge, U. Maheswari, T. Maurel, M. D. McDowall, B. Moore, M. Muffato, G. Naamati, S. Naithani, A. Olson, I. Papatheodorou, M. Patricio, M. Paulini, H. Pedro, E. Perry, J. Preece, M. Rosello, M. Russell, V. Sitnik, D.M. Staines, J. Stein, M.K. Tello-Ruiz, S. J. Trevanion, M. Urban, S. Wei, D. Ware, G. Williams, A.D. Yates, P. Flicek, Ensembl genomes 2020-enabling non-vertebrate genomic research, Nucleic Acids Res. 48 (2020) D689–D695, https://doi.org/10.1093/NAR/GKZ890.

[26] E. Gasteiger, C. Hoogland, A. Gattiker, S. Duvaud, M.R. Wilkins, R.D. Appel, A. Bairoch, Protein identification and analysis tools on the ExPASy server, in: The Proteomics Protocols Handbook, 2005, pp. 571–607, https://doi.org/10.1385/1-59259-890-0:571.

[27] T.L. Bailey, J. Johnson, C.E. Grant, W.S. Noble, The MEME suite, Nucleic Acids Res. 43 (2015) W39–W49, https://doi.org/10.1093/nar/gkv416.

[28] C. Chen, H. Chen, Y. Zhang, H.R. Thomas, M.H. Frank, Y. He, R. Xia, TBtools: an integrative toolkit developed for interactive analyses of big biological data, Mol. Plant 13 (2020) 1194–1202, https://doi.org/10.1016/J.MOLP.2020.06.009.

[29] C. Geourjon, G. Deléage, SOPMA: significant improvements in protein secondary structure prediction by consensus prediction from multiple alignments, Comput. Appl. Biosci. 11 (1995) 681–684, https://doi.org/10.1093/BIOINFORMATICS/ 11.6.681.

[30] L.A. Kelley, S. Mezulis, C.M. Yates, M.N. Wass, M.J.E. Sternberg, The Phyre2 web portal for protein modeling, prediction and analysis, Nat. Protoc. 10 (2015) 845–858, https://doi.org/10.1038/nprot.2015.053.

[31] M.N. Nguyen, K.P. Tan, M.S. Madhusudhan, CLICK—topology-independent comparison of biomolecular 3D structures, Nucleic Acids Res. 39 (2011) W24, https://doi.org/10.1093/NAR/GKR393.

[32] W. Tian, C. Chen, X. Lei, J. Zhao, J. Liang, CASTp 3.0: computed atlas of surface topography of proteins, Nucleic Acids Res. 46 (2018) W363–W367, https://doi. org/10.1093/NAR/GKY473.

[33] G.M. Morris, H. Ruth, W. Lindstrom, M.F. Sanner, R.K. Belew, D.S. Goodsell, A. J. Olson, AutoDock4 and AutoDockTools4: automated docking with selective receptor flexibility, J. Comput. Chem. 30 (2009) 2785–2791, https://doi.org/ 10.1002/JCC.21256.

[34] R.A. Laskowski, M.B. Swindells, LigPlot+: multiple ligand-protein interaction diagrams for drug discovery, J. Chem. Inf. Model. 51 (2011) 2778–2786, https:// doi.org/10.1021/ci200227u.

[35] R.C. Edgar, MUSCLE: multiple sequence alignment with high accuracy and high throughput, Nucleic Acids Res. 32 (2004) 1792–1797, https://doi.org/10.1093/ NAR/GKH340.

[36] S. Kumar, G. Stecher, M. Li, C. Knyaz, K. Tamura, MEGA X: molecular evolutionary genetics analysis across computing platforms, Mol. Biol. Evol. 35 (2018) 1547–1549, https://doi.org/10.1093/molbev/msy096.

[37] D.M. Emms, S. Kelly, OrthoFinder: phylogenetic orthology inference for comparative genomics, Genome Biol. 20 (2019) 1–14, https://doi.org/10.1186/ S13059-019-1832-Y.

[38] P. Shannon, A. Markiel, O. Ozier, N.S. Baliga, J.T. Wang, D. Ramage, N. Amin, B. Schwikowski, T. Idekar, Cytoscape: a software environment for integrated models of biomolecular interaction networks, Genome Res. 13 (2003) 2498–2504, https://doi.org/10.1101/gr.1239303.

[39] Y. Wang, H. Tang, J.D. Debarry, X. Tan, J. Li, X. Wang, T.H. Lee, H. Jin, B. Marler, H. Guo, J.C. Kissinger, A.H. Paterson, MCScanX: a toolkit for detection and evolutionary analysis of gene synteny and collinearity, Nucleic Acids Res. 40 (2012), https://doi.org/10.1093/NAR/GKR1293.

[40] Z. Gu, A. Cavalcanti, F.-C. Chen, P. Bouman, W.-H. Li, Extent of gene duplication in the genomes of Drosophila, nematode, and yeast, Mol. Biol. Evol. 19 (2002) 256–262, https://doi.org/10.1093/oxfordjournals.molbev.a004079.

[41] Z. Zhang, KaKs_calculator 3.0: calculating selective pressure on coding and non-coding sequences, Genomics Proteomics Bioinformatics (2022), https://doi.org/ 10.1016/J.GPB.2021.12.002, 2017 8:1.

[42] M.A. Koch, B. Haubold, T. Mitchell-Olds, Comparative evolutionary analysis of chalcone synthase and alcohol dehydrogenase loci in Arabidopsis, Arabis, and related genera (Brassicaceae), Mol. Biol. Evol. 17 (2000) 1483–1498, https://doi. org/10.1093/OXFORDJOURNALS.MOLBEV.A026248.

[43] M. Lescot, PlantCARE, a database of plant cis-acting regulatory elements and a portal to tools for in silico analysis of promoter sequences, Nucleic Acids Res. 30 (2002) 325–327, https://doi.org/10.1093/nar/30.1.325.

[44] F. Tian, D.C. Yang, Y.Q. Meng, J. Jin, G. Gao, PlantRegMap: charting functional regulatory maps in plants, Nucleic Acids Res. 48 (2020) D1104–D1113, https:// doi.org/10.1093/NAR/GKZ1020.

[45] X. Dai, P.X. Zhao, PsRNATarget: a plant small RNA target analysis server, Nucleic Acids Res. 39 (2011) 155–159, https://doi.org/10.1093/nar/gkr319.

[46] S. Gui, L. Yang, J. Li, J. Luo, X. Xu, J. Yuan, L. Chen, W. Li, X. Yang, S. Wu, S. Li, Y. Wang, Y. Zhu, Q. Gao, N. Yang, J. Yan, ZEAMAP, a comprehensive database adapted to the maize multi-omics era, IScience 23 (2020), 101241, https://doi. org/10.1016/J.ISCI.2020.101241.

[47] T. Obayashi, H. Hibara, Y. Kagaya, Y. Aoki, K. Kinoshita, ATTED-II v11: a plant gene coexpression database using a sample balancing technique by subagging of principal components, Plant Cell Physiol. 63 (2022) 869–881, https://doi.org/ 10.1093/PCP/PCAC041.

[48] K. Arora, K.K. Panda, S. Mittal, M.G. Mallikarjuna, N. Thirunavukkarasu, In silico characterization and functional validation of cell wall modification genes imparting waterlogging tolerance in maize, Bioinform. Biol. Insights 11 (2017), https://doi.org/10.1177/1177932217744277.

[49] H. van Gioi, M.G. Mallikarjuna, M. Shikha, B. Pooja, S.K. Jha, P.K. Dash, A. M. Basappa, R.N. Gadag, A.R. Rao, T. Nepolean, Variable level of dominance of candidate genes controlling drought functional traits in maize hybrids, Front. Plant Sci. 8 (2017), https://doi.org/10.3389/fpls.2017.00940.

[50] M.G. Mallikarjuna, R. Sharma, P. Veeraya, A. Tyagi, A.R. Rao, L. Hirenallur Chandappa, V. Chinnusamy, Evolutionary and functional characterisation of glutathione peroxidases showed splicing mediated stress responses in maize, Plant Physiol. Biochem. 178 (2022) 40–54, https://doi.org/10.1016/J. PLAPHY.2022.02.024.

[51] K.J. Livak, T.D. Schmittgen, Analysis of relative gene expression data using real-time quantitative PCR and the 2−ΔΔCT method, Methods 25 (2001) 402–408, https://doi.org/10.1006/meth.2001.1262.

[52] M. Guo, M.A. Rupe, O.N. Danilevskaya, X. Yang, Z. Hu, Genome-wide mRNA profiling reveals heterochronic allelic variation and a new imprinted gene in hybrid maize endosperm, Plant J. 36 (2003) 30–44, https://doi.org/10.1046/ j.1365-313X.2003.01852.x.

[53] M. Guo, M.A. Rupe, X. Yang, O. Crasta, C. Zinselmeier, O.S. Smith, B. Bowen, Genome-wide transcript analysis of maize hybrids: allelic additive gene expression and yield heterosis, Theor. Appl. Genet. 113 (2006) 831–845, https:// doi.org/10.1007/s00122-006-0335-x.

[54] A. Liu, C. Liu, H. Lei, Z. Wang, M. Zhang, X. Yan, G. Yang, J. Ren, Phylogenetic analysis and transcriptional profiling of WRKY genes in sunflower (Helianthus annuus L.): genetic diversity and their responses to different biotic and abiotic stresses, Ind. CropsProd. 148 (2020), 112268, https://doi.org/10.1016/J. INDCROP.2020.112268.

[55] H. Mizuno, S. Kasuga, H. Kawahigashi, The sorghum SWEET gene family: stem sucrose accumulation as revealed through transcriptome profiling, Biotechnol. Biofuels 9 (2016) 1–12, https://doi.org/10.1186/S13068-016-0546-6.

[56] J.S. Eom, L.Q. Chen, D. Sosso, B.T. Julius, I.W. Lin, X.Q. Qu, D.M. Braun, W. B. Frommer, SWEETs, transporters for intracellular and intercellular sugar translocation, Curr. Opin. Plant Biol. 25 (2015) 53–62, https://doi.org/10.1016/ J.PBI.2015.04.005.

[57] L.Q. Chen, X.Q. Qu, B.H. Hou, D. Sosso, S. Osorio, A.R. Fernie, W.B. Frommer, Sucrose efflux mediated by SWEET proteins as a key step for phloem transport, Science 335 (2012) 207–211, https://doi.org/10.1126/SCIENCE.1213351.

[58] N. Singh, M. Ujinwal, S. Langyan, R.Z. Sayyed, H.A. el Enshasy, A.A. Kenawy, Genome-wide exploration of sugar transporter (sweet) family proteins in Fabaceae for sustainable protein and carbon source, PLoS One 17 (2022), e0268154, https://doi.org/10.1371/JOURNAL.PONE.0268154.

[59] H. Miao, P. Sun, Q. Liu, Y. Miao, J. Liu, K. Zhang, W. Hu, J. Zhang, J. Wang, Z. Wang, C. Jia, B. Xu, Z. Jin, Genome-wide analyses of SWEET family proteins reveal involvement in fruit development and abiotic/biotic stress responses in banana, Sci. Rep. 7 (2017) 1–15, https://doi.org/10.1038/s41598-017-03872-w, 2017 7:1.

[60] T. Gautam, T. Saripalli, V. Gahlaut, A. Kumar, P.K. Sharma, H.S. Balyan, P. K. Gupta, Further studies on sugar transporter (SWEET) genes in wheat (Triticum aestivum L.), Mol. Biol. Rep. 46 (2019) 2327–2353, https://doi.org/10.1007/ S11033-019-04691-0.

[61] S.E. O'Connor, B. Imperiali, Modulation of protein structure and function by asparagine-linked glycosylation, Chem. Biol. 3 (1996) 803–812, https://doi.org/ 10.1016/S1074-5521(96)90064-2.

[62] E. Weerapana, B. Imperiali, Asparagine-linked protein glycosylation: from eukaryotic to prokaryotic systems, Glycobiology 16 (2006), https://doi.org/ 10.1093/GLYCOB/CWJ099.

[63] N. Shukla, E. Pomarico, C.J.S. Hecht, E.A. Taylor, M. Chergui, C.M. Othon, Hydrophobic interactions of sucralose with protein structures, Arch. Biochem. Biophys. 639 (2018) 38–43, https://doi.org/10.1016/J.ABB.2017.12.013.

[64] U. Fatima, D. Balasubramaniam, W.A. Khan, M. Kandpal, J. Vadassery, A. Arockiasamy, M. Senthil-Kumar, SWEET11 and SWEET12 Transporters Function in Tandem to Modulate Sugar Flux in Arabidopsis: An Account of the Underlying Unique Structure–Function Relationship, BioRxiv, 2022, https://doi.org/10.1101/2022.03.26.485957, 2022.03.26.485957.

[65] Y. Tao, L.S. Cheung, S. Li, J.S. Eom, L.Q. Chen, Y. Xu, K. Perry, W.B. Frommer, L. Feng, Structure of a eukaryotic SWEET transporter in a homotrimeric complex, Nature 527 (2015) 259–263, https://doi.org/10.1038/nature15391, 2015 10:6.

[66] H. Guo, Y. Jiao, X. Tan, X. Wang, X. Huang, H. Jin, A.H. Paterson, Gene duplication and genetic innovation in cereal genomes, Genome Res. 29 (2019) 261–269, https://doi.org/10.1101/GR.237511.118.

[67] Y.T. Kuo, Y.T. Chao, W.C. Chen, M.C. Shih, S.bin Chang, Segmental and tandem chromosome duplications led to divergent evolution of the chalcone synthase gene family in Phalaenopsis orchids, Ann. Bot. 123 (2019) 69–77, https://doi.org/10.1093/AOB/MCY136.

[68] Y. Cheng, X. Li, H. Jiang, W. Ma, W. Miao, T. Yamada, M. Zhang, Systematic analysis and comparison of nucleotide-binding site disease resistance genes in maize, FEBS J. 279 (2012) 2431–2443, https://doi.org/10.1111/J.1742-4658.2012.08621.X.

[69] Y. Zhao, Y. Zhou, H. Jiang, X. Li, D. Gan, X. Peng, S. Zhu, B. Cheng, Systematic analysis of sequences and expression patterns of drought-responsive members of the HD-zip gene family in maize, PLoS One 6 (2011), e28488, https://doi.org/10.1371/JOURNAL.PONE.0028488.

[70] Q. Wang, J. Liu, Y. Wang, Y. Zhao, H. Jiang, B. Cheng, Systematic analysis of the maize PHD-finger gene family reveals a subfamily involved in abiotic stress response, Int. J. Mol. Sci. 16 (2015) 23517–23544, https://doi.org/10.3390/IJMS161023517.

[71] S.B. Cannon, A. Mitra, A. Baumgarten, N.D. Young, G. May, The roles of segmental and tandem gene duplication in the evolution of large gene families in Arabidopsis thaliana, BMC Plant Biol. 4 (2004) 10, https://doi.org/10.1186/1471-2229-4-10.

[72] M. Degiorgio, R. Assis, Learning retention mechanisms and evolutionary parameters of duplicate genes from their expression data, Mol. Biol. Evol. 38 (2021) 1209–1224, https://doi.org/10.1093/MOLBEV/MSAA267.

[73] S.L. Liu, G.J. Baute, K.L. Adams, Organ and cell type-specific complementary expression patterns and regulatory neofunctionalization between duplicated genes in Arabidopsis thaliana, Genome Biol. Evol. 3 (2011) 1419–1436, https://doi.org/10.1093/GBE/EVR114.

[74] C. Zou, M.D. Lehti-Shiu, M. Thomashow, S.H. Shiu, Evolution of stress-regulated gene expression in duplicate genes of Arabidopsis thaliana, PLoS Genet. 5 (2009), e1000581, https://doi.org/10.1371/JOURNAL.PGEN.1000581.

[75] T.E. Hughes, J.A. Langdale, S. Kelly, The impact of widespread regulatory neofunctionalization on homeolog gene evolution following whole-genome duplication in maize, Genome Res. 24 (2014) 1348, https://doi.org/10.1101/GR.172684.114.

[76] J. Lai, Gene loss and movement in the maize genome, Genome Res. 14 (2004) 1924–1931, https://doi.org/10.1101/gr.2701104.

[77] B. Linard, I. Ebersberger, S.E. McGlynn, N. Glover, T. Mochizuki, M. Patricio, O. Lecompte, Y. Nevers, P.D. Thomas, T. Gabaldon, E. Sonnhammer, C. Dessimoz, I. Uchiyama, A. Altenhoff, A. Ouangraoua, A.W. Vesztrocy, B. Linard, C. Dessimoz, D. Szklarczyk, D. Durand, D. Emms, D. Moi, D. Thybert, E. Sonnhammer, E. Kriventseva, H. Tang, H. Chiba, I. Uchiyama, I. Ebersberger, J. Huerta-Cepas, J.T. Fernandez-Breis, J.A. Blake, L. Pryszcz, M.J. Martin, M. M. Houben, M. Patricio, M. Muffato, N. Glover, O. Lecompte, P.D. Thomas, P. Schiffer, S. Capella-Gutierrez, S. Cosentino, S.E. McGlynn, S. Kuraku, S. Forslund, S. Kelly, S. Lewis, T. Jones, T.M. de Farias, T. Maeda, W. Iwasaki, W. Pearson, Y. Wang, Y. Nevers, Y. Hara, Ten years of collaborative progress in the quest for orthologs, Mol. Biol. Evol. 38 (2021) 3033–3045, https://doi.org/10.1093/MOLBEV/MSAB098.

[78] M. Remm, C.E.V. Storm, E.L.L. Sonnhammer, Automatic clustering of orthologs and in-paralogs from pairwise species comparisons, J. Mol. Biol. 314 (2001) 1041–1052, https://doi.org/10.1006/JMBI.2000.5197.

[79] G. Fang, N. Bhardwaj, R. Robiotto, M.B. Gerstein, Getting started in gene orthology and functional analysis, PLoS Comput. Biol. 6 (2010), e1000703, https://doi.org/10.1371/JOURNAL.PCBI.1000703.

[80] I. Wapinski, A. Pfeffer, N. Friedman, A. Regev, Natural history and evolutionary principles of gene duplication in fungi, Nature 449 (2007) 54–61, https://doi.org/10.1038/NATURE06107.

[81] I. Cvijović, B.H. Good, M.M. Desai, The effect of strong purifying selection on genetic diversity, Genetics 209 (2018) 1235, https://doi.org/10.1534/GENETICS.118.301058.

[82] M. Bezrutczyk, T. Hartwig, M. Horschman, S.N. Char, J. Yang, B. Yang, W. B. Frommer, D. Sosso, Impaired phloem loading in zmsweet13a,b,c sucrose transporter triple knock-out mutants in Zea mays, New Phytol. 218 (2018) 594–603, https://doi.org/10.1111/NPH.15021.

[83] J. Yang, D. Luo, B. Yang, W.B. Frommer, J.S. Eom, SWEET11 and 15 as key players in seed filling in rice, New Phytol. 218 (2018) 604–615, https://doi.org/10.1111/NPH.15004.

[84] Z. Chu, M. Yuan, J. Yao, X. Ge, B. Yuan, C. Xu, X. Li, B. Fu, Z. Li, J.L. Bennetzen, Q. Zhang, S. Wang, Promoter mutations of an essential gene for pollen development result in disease resistance in rice, Genes Dev. 20 (2006) 1250–1255, https://doi.org/10.1101/GAD.1416306.

[85] P. Gebauer, M. Korn, T. Engelsdorf, U. Sonnewald, C. Koch, L.M. Voll, Sugar accumulation in leaves of arabidopsis sweet11/sweet12 double mutants enhances priming of the salicylic acid-mediated defense response, Front. Plant Sci. 8 (2017) 1378, https://doi.org/10.3389/FPLS.2017.01378.

[86] J. Kottapalli, R. David-Schwartz, B. Khamaisi, D. Brandsma, N. Lugassi, A. Egbaria, G. Kelly, D. Granot, Sucrose-induced stomatal closure is conserved across evolution, PLoS One 13 (2018), e0205359, https://doi.org/10.1371/JOURNAL.PONE.0205359.

[87] Q. Chen, T. Hu, X. Li, C.P. Song, J.K. Zhu, L. Chen, Y. Zhao, Phosphorylation of SWEET sucrose transporters regulates plant root:shoot ratio under drought, Nat. Plants 8 (2021) 68–77, https://doi.org/10.1038/s41477-021-01040-7, 2022 8:1.

[88] J. Mathan, A. Singh, A. Ranjan, Sucrose transport in response to drought and salt stress involves ABA-mediated induction of OsSWEET13 and OsSWEET15 in rice, Physiol. Plant. 171 (2021) 620–637, https://doi.org/10.1111/PPL.13210.

[89] R.K. Jha, J. Patel, M.K. Patel, A. Mishra, B. Jha, Introgression of a novel cold and drought regulatory-protein encoding CORA-like gene, SbCDR, induced osmotic tolerance in transgenic tobacco, Physiol. Plant. 172 (2021) 1170–1188, https://doi.org/10.1111/PPL.13280.

[90] T. Saminathan, A. Alvarado, C. Lopez, S. Shinde, B. Gajanayake, V.L. Abburi, V. G. Vajja, G. Jagadeeswaran, K. Raja Reddy, P. Nimmakayala, U.K. Reddy, Elevated carbon dioxide and drought modulate physiology and storage-root development in sweet potato by regulating microRNAs, Funct. Integr. Genomics 19 (2019) 171–190, https://doi.org/10.1007/S10142-018-0635-7.

[91] M. Şahin-Çevik, B. Çevik, A. Coşkan, Identification and expression analysis of salinity-induced genes in Rangpur lime (Citrus limonia), Hortic Plant J. 6 (2020) 267–276, https://doi.org/10.1016/J.HPJ.2020.07.005.

[92] J. Danyluk, A. Perron, M. Houde, A. Limin, B. Fowler, N. Benhamou, F. Sarhan, Accumulation of an acidic dehydrin in the vicinity of the plasma membrane during cold acclimation of wheat, Plant Cell 10 (1998) 623–638, https://doi.org/10.1105/TPC.10.4.623.

[93] T. Horie, F. Hauser, J.I. Schroeder, HKT transporter-mediated salinity resistance mechanisms in Arabidopsis and monocot crop plants, Trends Plant Sci. 14 (2009) 660, https://doi.org/10.1016/J.TPLANTS.2009.08.009.

[94] N. Uozumi, E.J. Kim, F. Rubio, T. Yamaguchi, S. Muto, A. Tsuboi, E.P. Bakker, T. Nakamura, J.I. Schroeder, The Arabidopsis HKT1 gene homolog mediates inward Na(+) currents in Xenopus laevis oocytes and Na(+) uptake in Saccharomyces cerevisiae, Plant Physiol. 122 (2000) 1249–1259, https://doi.org/10.1104/PP.122.4.1249.

[95] Z.H. Ren, J.P. Gao, L.G. Li, X.L. Cai, W. Huang, D.Y. Chao, M.Z. Zhu, Z.Y. Wang, S. Luan, H.X. Lin, A rice quantitative trait locus for salt tolerance encodes a sodium transporter, Nat. Genet. 37 (2005) 1141–1146, https://doi.org/10.1038/ng1643, 2005 37:10.

[96] D. Kumutha, R.K. Sairam, K. Ezhilmathi, V. Chinnusamy, R.C. Meena, Effect of waterlogging on carbohydrate metabolism in pigeon pea (Cajanus cajan L.): upregulation of sucrose synthase and alcohol dehydrogenase, Plant Sci. 175 (2008) 706–716, https://doi.org/10.1016/J.PLANTSCI.2008.07.013.

[97] R.K. Sarkar, A. Ray, Submergence-tolerant rice withstands complete submergence even in saline water: probing through chlorophyll a fluorescence induction O-J-I-P transients, Photosynthetica 54 (2015) 275–287, https://doi.org/10.1007/S11099-016-0082-4, 2016 54:2.

[98] X. Qi, Q. Li, J. Shen, C. Qian, X. Xu, Q. Xu, X. Chen, Sugar enhances waterlogging-induced adventitious root formation in cucumber by promoting auxin transport and signalling, Plant Cell Environ. 43 (2020) 1545–1557, https://doi.org/10.1111/PCE.13738.

[99] U.J. Phukan, G.S. Jeena, V. Tripathi, R.K. Shukla, MaRAP2-4, a waterlogging-responsive ERF from Mentha, regulates bidirectional sugar transporter AtSWEET10 to modulate stress response in Arabidopsis, Plant Biotechnol. J. 16 (2018) 221–233, https://doi.org/10.1111/PBI.12762.

[100] C.X. Zhang, B.H. Feng, T.T. Chen, W.M. Fu, H.B. Li, G.Y. Li, Q.Y. Jin, L.X. Tao, G. F. Fu, Heat stress-reduced kernel weight in rice at anthesis is associated with impaired source-sink relationship and sugars allocation, Environ. Exp. Bot. 155 (2018) 718–733, https://doi.org/10.1016/J.ENVEXPBOT.2018.08.021.

[101] H. Yang, X. Gu, M. Ding, W. Lu, D. Lu, Heat stress during grain filling affects activities of enzymes involved in grain protein and starch synthesis in waxy maize, Sci. Rep. 8 (2018) 1–9, https://doi.org/10.1038/s41598-018-33644-z, 2018 8:1.

[102] J. Zhang, X. Jiang, T. Li, T. Chang, Effect of elevated temperature stress on the production and metabolism of photosynthate in tomato (Lycopersicon esculentum L.) leaves, J. Hortic. Sci. Biotechnol. 87 (2015) 293–298, https://doi.org/10.1080/14620316.2012.11512867.

[103] C.A. Ferreira De Sousa, L. Sodek, C.A.F. Sousa, L. Sodek, The metabolic response of plants to oxygen deficiency, Braz. J. Plant Physiol. 14 (2002) 83–94, https://doi.org/10.1590/S1677-04202002000200002.

[104] X. Ma, F. Xing, Q. Jia, Q. Zhang, T. Hu, B. Wu, L. Shao, Y. Zhao, Q. Zhang, D. X. Zhou, Parental variation in CHG methylation is associated with allelic-specific expression in elite hybrid rice, Plant Physiol. 186 (2021) 1025–1041, https://doi.org/10.1093/PLPHYS/KIAB088.

[105] S. Meyer, H. Pospisil, S. Scholten, Heterosis associated gene expression in maize embryos 6 days after fertilization exhibits additive, dominant and overdominant pattern, Plant Mol. Biol. 63 (2007) 381–391, https://doi.org/10.1007/S11103-006-9095-X.

[106] F. Hochholdinger, N. Hoecker, Towards the molecular basis of heterosis, Trends Plant Sci. 12 (2007) 427–432, https://doi.org/10.1016/J.TPLANTS.2007.08.005.

[107] R. Song, J. Messing, Gene expression of a gene family in maize based on noncollinear haplotypes, Proc. Natl. Acad. Sci. U. S. A. 100 (2003) 9055–9060, https://doi.org/10.1073/PNAS.1032999100.

[108] N.M. Springer, K. Ying, Y. Fu, T. Ji, C.T. Yeh, Y. Jia, W. Wu, T. Richmond, J. Kitzman, H. Rosenbaum, A.L. Iniguez, W.B. Barbazuk, J.A. Jeddeloh, D. Nettleton, P.S. Schnable, Maize inbreds exhibit high levels of copy number variation (CNV) and Presence/Absence variation (PAV) in genome content, PLoS Genet. 5 (2009), e1000734, https://doi.org/10.1371/JOURNAL.PGEN.1000734.

[109] W. Yuan, F. Beitel, T. Srikant, I. Bezrukov, S. Schäfer, R. Kraft, D. Weigel, Pervasive Under-Dominance in Gene Expression as Unifying Principle of Biomass Heterosis in Arabidopsis, BioRxiv, 2022, https://doi.org/10.1101/2022.03.03.482808, 2022.03.03.482808.

[110] G. Gibson, R. Riley-Berger, L. Harshman, A. Kopp, S. Vacha, S. Nuzhdin, M. Wayne, Extensive sex-specific nonadditivity of gene expression in Drosophila melanogaster, Genetics 167 (2004) 1791–1799, https://doi.org/10.1534/genetics.104.026583.

[111] M. Vuylsteke, F. van Eeuwijk, P. van Hummelen, M. Kuiper, M. Zabeau, Genetic analysis of variation in gene expression in Arabidopsis thaliana, Genetics 171 (2005) 1267–1275, https://doi.org/10.1534/genetics.105.041509.

[112] R.M. Stupar, J.M. Gardiner, A.G. Oldre, W.J. Haun, V.L. Chandler, N.M. Springer, Gene expression analyses in maize inbreds and hybrids with varying levels of heterosis, BMC Plant Biol. 8 (2008) 33, https://doi.org/10.1186/1471-2229-8-33.

[113] R.J. Schmitz, E. Grotewold, M. Stam, Cis-regulatory sequences in plants: their importance, discovery, and future challenges, Plant Cell 34 (2022) 718–741, https://doi.org/10.1093/PLCELL/KOAB281.

[114] M. Guo, M.A. Rupe, C. Zinselmeier, J. Habben, B.A. Bowen, O.S. Smith, Allelic variation of gene expression in maize hybrids, Plant Cell 16 (2004) 1707–1716, https://doi.org/10.1105/tpc.022087.

[115] J. Rohrmann, R. McQuinn, J.J. Giovannoni, A.R. Fernie, T. Tohge, Tissue specificity and differential expression of transcription factors in tomato provide hints of unique regulatory networks during fruit ripening, Plant Signal. Behav. 7 (2012) 1639, https://doi.org/10.4161/PSB.22264.

[116] R.A. Swanson-Wagner, Y. Jia, R. DeCook, L.A. Borsuk, D. Nettleton, P.S. Schnable, All possible modes of gene action are observed in a global comparison of gene expression in a maize F 1 hybrid and its inbred parents, Proc. Natl. Acad. Sci. 103 (2006) 6805–6810, https://doi.org/10.1073/pnas.0510430103.

[117] E.B. Sepúlveda-García, J.F. Pulido-Barajas, A.A. Huerta-Heredia, J.M. Peña-Castro, R. Liu, B.E. Barrera-Figueroa, Differential expression of maize and teosinte microRNAs under submergence, drought, and alternated stress, Plants (Basel) 9 (2020) 1–20, https://doi.org/10.3390/PLANTS9101367.

[118] C.M. Seeve, R. Sunkar, Y. Zheng, L. Liu, Z. Liu, M. McMullen, S. Nelson, R. E. Sharp, M.J. Oliver, Water-deficit responsive microRNAs in the primary root growth zone of maize, BMC Plant Biol. 19 (2019) 1–16, https://doi.org/10.1186/S12870-019-2037-Y.